Universidade de Aveiro Departamento de Química

Ano 2019

Mafalda Dias de Campos Neto

Produção de micropartículas bidimensionais (2D) com geometria controlada usando plataformas de elevado contraste de molhabilidade

Fabrication of two-dimensional (2D) shape-tailored microparticles using wettability contrast-based platforms

Universidade de Aveiro Departamento de Química
Ano 2019

Mafalda Dias de Campos Neto

Produção de micropartículas bidimensionais (2D) com geometria controlada usando plataformas de elevado contraste de molhabilidade

Fabrication of two-dimensional (2D) shape-tailored microparticles using wettability contrast-based platforms

Tese apresentada à Universidade de Aveiro para cumprimento dos requisitos necessários à obtenção do grau de Mestre em Biotecnologia Molecular, realizada sob a orientação científica da Doutora Mariana Braga de Oliveira, Investigadora Júnior e do Professor Doutor João Filipe Colardelle da Luz Mano, Professor Catedrático do Departamento de Química da Universidade de Aveiro

“It does not matter how slowly you go as long as you do not stop.”

– Confucius

o júri

presidente	Professora Doutora Luísa Alexandra Seuanes Serafim Martins Leal Professora Auxiliar do Departamento de Química da Universidade de Aveiro
vogal – arguente principal	Doutora Liliana Inácio Bernardino Professora Auxiliar do Departamento de Ciências Médicas da Universidade da Beira Interior
vogal – orientador	Doutora Mariana Braga de Oliveira Investigadora Júnior, Laboratório Associado CICECO – Instituto de Materiais da Universidade de Aveiro

acknowledgments

First of all, I would like to express my gratitude and appreciation to Prof. João Mano for welcoming me into the COMPASS Group and for the opportunity to work towards my final project of my Master's degree, without whom this work could never be accomplished, and, of course, for providing me with the best tools and equipment necessary for its success.

Secondly, I would like to acknowledge the forever guidance of Mariana Oliveira throughout my whole journey, especially the perseverance and endurance that she transmitted and taught me to have. In times of doubt and insecurity she never let me give up and encouraged me into keep my head up and fight.

I would also like to bless my whole family, who always stood by my side no matter what, and whose unconditional love guided me through my 'bumpy road". Especially, my biggest gratitude to my dearest mother and aunt, who accompanied me since day one and know me from head to toe, and inside out. My appreciation will never be well expressed with only these simple and basic words. They mean the world to me and I will be forever grateful for everything they have ever done to me.

I cannot but offer my heartfelt gratitude to Tamagno, who revealed to be the most sweet and pleasant surprise inside these box of chocolates, that is my life. They say that we never know which one we are going to get, but lucky me. To all the late night talks and working hours, to all the support and help, to all the moments we shared.

To all members of the COMPASS Group and co-workers a huge thank you, especially to Maria Clara Gomes, who jumped in unexpectedly into this project but instantly showed a big commitment, and always offered any help that she could give.

To João, who always showed his support and never stopped believing me, and my work. One of the most pure souls I could came across in my entire life. And my fellow companions whose friendship I would always keep in my heart.

Finally, I would like to thanks Filipe Oliveira and Miguel Neto who were always helpful and available to spend countless hours in the Profilometry just to respond to my needs.

palavras-chave

design de micropartículas, carriers avançados de células, partículas poliméricas ultra-finas, superfícies padronizadas, contrastes de molhabilidade

resumo

Durante várias décadas, as micropartículas têm sido usadas como veículos esféricos para a entrega controlada de fármacos ou mesmo como *carriers* para a expansão celular em larga escala. Mais recentemente, estas estruturas têm recebido uma grande atenção em diversas áreas da bioengenharia, podendo integrar uma vasta variedade de estratégias que incluem, não só, a engenharia de tecidos, como também *bioprinting* 3D ou mesmo o desenvolvimento de modelos de tecidos/doença. O conceito de micropartículas esféricas como suportes adequados à cultura e expansão celular têm sido contestados se serão a abordagem mais adequada. Para tal, sistemas que sejam capazes de alterar não só a geometria, mas também modelar as propriedades (bio)químicas e físicas, são fatores determinantes em diversas tecnologias. Neste sentido, a descoberta de materiais 2D levou a um rápido aparecimento de uma diversidade de estruturas que exibem propriedades únicas, como o (i) elevado rácio superfície de área-volume, (ii) espessuras à escala sub-micrométrica, (iii) a possibilidade de serem heterofuncionalizadas e ainda (iv) propriedades adesivas não covalentes, que se distinguem grandemente dos seus equivalentes 3D. Embora o desenvolvimento destas estruturas com dimensões laterais e geometrias flexíveis permaneça um desafio, plataformas baseadas em padrões têm permitido ultrapassar esta desvantagem. Por esta razão, neste trabalho, superfícies com elevado contraste de molhabilidade foram utilizadas para o fabrico de partículas com diferentes tamanhos e formas (quadrados, círculos, triângulos e hexágonos), apresentando uma espessura à escala nanométrica. Ademais, estas partículas ultra-finas quando em contacto com células estaminais derivadas do tecido adiposo permitem a formação de esferóides sem impedir a sua normal agregação e morfologia. As células mantiveram-se viáveis e metabolicamente ativas durante os 3 dias de cultura, e verificou-se ainda, um aumento na libertação de fatores angiogénicos (VEGF).

keywords microparticle design, advanced cell carriers, ultra-thin polymeric particles, patterned surfaces, wettable-dewettable contrasts

abstract For several decades microparticles have been exclusively and extensively explored as spherical drug delivery vehicles and large-scale cell expansion carriers. More recently, microparticulate structures gained interest in broader bioengineering fields, integrating a myriad of strategies that include bottom-up tissue engineering, three-dimensional (3D) bioprinting, and development of tissue/disease models. The concept of bulk spherical micrometric particles as adequate supports for cell culture has been challenged, and systems with finely tuned geometric designs and (bio)chemical/physical features are current key players in impacting technologies. In this sense, the discovery of two-dimensional (2D) materials led to the breakthrough of a multitude of different low dimensional structures with very unique properties, namely (i) high surface area-to-volume ratio, (ii) sub-micrometer thickness, (iii) heterofunctionality and (iv) non-covalent adhesiveness, which surpass their bulk counterparts. Although their development regarding tunable lateral-dimensions and geometries remains challenging, pre-patterned platforms had gain significant attention in addressing such drawback. Herein, resorting to wettability contrast patterned surfaces, different nanometer-thick particles of various sizes and geometries (e.g. squares, circles, triangles, hexagons) with high precision and definition were developed. These ultrathin quasi-2D polymeric microparticles in contact with cells allow the generation of gravity-enforced human adipose-derived stems cells spheroids without impairing their natural morphology. Cell culture for 3 days maintain cells viable, metabolically active and an increase in the release of angiogenic factors, namely VEGF.

Table of Contents

CHAPTER I – Introduction

CHAPTER II – Materials and Methods

CHAPTER III – Results and Discussion

CHAPTER IV – Conclusions and Future Perspectives

SUPPORTING INFORMATION

List of Figures

CHAPTER I – Introduction

CHAPTER II – Materials and Methods

CHAPTER III – Results and Discussion

SUPPORTING INFORMATION

List of Tables

CHAPTER I – Introduction

List of Abbreviations and Acronyms

#	
2D	Two-dimensional
3D	Three-dimensional
α-MEM	Minimum essential medium α-modification
A	
ASC	Adipose-derived mesenchymal stem cell
B	
bFGF	Basic fibroblast growth factor
C	
Ca-polyP	Calcium polyphosphate
CAM	Cellular adhesion molecule
CDMVS	Chloro(dimethyl)vinylsilane
CLSM	Confocal Laser Scanning Microscopy
Coum-6	Coumarin-6
D	
DAPI	4’,6-diamidino-2-phenylindole
DCM	Dichloromethane
DEAE	Diethylaminoethyl
DMAP	4-(Dimethylamino)pyridine
DPBS	Dulbecco’s phosphate-buffered saline
E	
ECM	Extracellular matrix
EDTA	Ethylenediaminetetracetic acid
ELISA	Enzyme-linked Immunosorbent Assay
EtOH	Ethanol

F

FBS	Fetal Bovine Serum

G

GF	Growth factor

H

H_2SO_4	Sulfuric acid
HA	Hyaluronic acid
HTS	High-throughput screening
HUVEC	Human umbilical vein endothelial cell

L

LbL	Layer-by-Layer

M

M_n	Number average molecular weight
MSC	Mesenchymal stem cell

N

NaOH	Sodium Hydroxide

P

PAA	Poly acrylic acid
PCL	Poly-ε-caprolactone
PDI	Polydispersity index
PDG-BB	Platelet-derived growth factor BB
PDMS	Polydimethylsiloxane
PEG	Polyethylene glycol
PEG-DA	Polyethylene glycol diacrilate
PFDT	1H,1H,2H,2H-Perfluorodecanethiol
PHA	Polyhydroxyalkanoate
PI	Propidium Iodide

PLA	Polylactic acid
PLGA	Polylactic-co-glycolic acid
PLL	Poly-L-lysine
PolyP	Polyphosphate
PS	Polystyrene
PSI	Phase-Shift Interferometer

R

RGD	Arginylglycylaspartic acid
RT	Room temperature
RWV	Rotate wall vessel

S

SA	Superamphiphobic
s.d.	Standard Deviation
SEM	Scanning Electron Microscopy
SH	Superhydrophobic
SL	Superhydrophilic

T

TEA	Triethylamine
TGF-β1	Transforming growth factor β1
THF	Tetrahydrofuran

U

UV	Ultraviolet

V

VEGF	Vascular endothelial growth factor

Chapter I*

Introduction

*This first chapter is based on the review article entitled
"Microparticles in Contact with Cells: from carriers to multifunctional tissue modulators"
(Trends Biotechnol., 2019, 37, 9, 1011-1028; DOI: 10.1016/j.tibtech.2019.02.008)

Microparticles in Contact with Cells: from carriers to multifunctional tissue modulators

Mafalda D. Neto[1], Mariana B. Oliveira[1,*], João F. Mano[1,*]

[*]Correspondence: M.B. Oliveira: mboliveira@ua.pt; J.F. Mano: jmano@ua.pt

[1]Department of Chemistry, CICECO – Aveiro Institute of Materials. University of Aveiro. Campus Universitário de Santiago. 3810-193 Aveiro, Portugal

I.1. Abstract

For several decades microparticles have been exclusively and extensively explored as spherical drug delivery vehicles and large-scale cell expansion carriers. More recently, microparticulate structures gained interest in broader bioengineering fields, integrating a myriad of strategies that include (i) bottom-up tissue engineering, (ii) three-dimensional (3D) bioprinting, and (iii) development of tissue/disease models. The concept of bulk spherical micrometric particles as adequate supports for cell cultivation has been challenged, and systems with finely tuned geometric designs and (bio)chemical/physical features are current key players in impacting technologies. Herein, we critically review the state of the art and future trends of biomaterial microparticles in contact with cells and tissues, excluding internalization studies, and with emphasis on innovative particles' design and applications.

Keywords: microparticle design, bottom-up tissue engineering, building-blocks, *in vitro* 3D models, bioinks, advanced microcarriers

I.2. Glossary

3D printing: additive manufacturing enabled by computer-aided technology that allows the precise deposition of a binder material into a complex architectural structure in a layer-by-layer logic.

3D Spheroids: spherical-shaped multicellular aggregates with improved cell-cell and cell-extracellular matrix (ECM) interactions, closely mimicking the microenvironment found in *in vivo* tissues.

Bioink: a liquid/viscous biomaterial that may contain cells and/or biological molecules which is processed by bioprinting technology through material extrusion and deposition into a spatially controlled pattern, during which its viscosity and elastic character will increase.

Bioinstructive: with the ability to influence the behaviour of biological systems, including cells and tissues.

Capsules: a closed-like system separated from the outer environment by a membrane barrier – shell – surrounding a core that can be presented as liquid, hollow or matrix composed.

Cell Stacking: methodology for cell expansion based on the parallel growth of cells on piled up tissue culture flasks.

High-Throughput Screening: methods that allow a fast acquisition, processing and analyses of large amounts of data.

Injectable scaffold: supporting matrix that possesses suitable physical and mechanical properties to be injected through a syringe or a catheter and to perfectly fit and fill a certain defect without the need of invasive interventions.

Microcarrier: supporting matrix characterized by a high surface area-to- volume ratio, allowing large-scale expansion of anchorage-dependent cells and *in vitro* production of biologically-active molecules.

Microparticle: micrometric sized (ranging 1-1000 μm) particle that is extensively used in biotechnological and biomedical fields as drug/cell-delivery platforms.

Modular Tissue Engineering: engineering of hierarchical and biologically-functional structures with precise architectural features through assembly of modular building-blocks using a bottom-up approach.

Multi-compartmentalized particles: biomaterial within the micrometric size range comprising architectural features that enable different chemical compositions over its spatial extension. Well-established examples of multicompartmental particles include Janus particles and co-axial multilayer (onion-like) particles.

Off-the-shelf: amenable to be used directly without any substantial handling, and "as is", independently from any establishment of settings during a pre-order procedure.

On-demand: an action that is dependent on the application of external stimulus/stimuli by the user.

Organoid: *in vitro* miniaturized organ with self-organized organ-specific cell types in an accurate spatial manner that are able to replicate physiological functions.

Tethered: attached/immobilized onto a surface.

Xeno-free: free of xenogeneic (originated from a different species) or animal derived-components.

I.3. Highlights

Promising outputs have been delivered by microparticles as microcarriers with enhanced surface area in response to high cellular demands. However, their ability to adapt to clinically translatable setups, including xeno-free conditions and the use of biodegradable materials, is still a leading-edge trend.

Advances in particle design and control over their architecture and morphology, along with understanding the role of tailorable (bio)chemical/physical aspects enables the modulation of cellular response. Finely tailored systems may be attained through several enabling technologies and fabrication methods.

Recent applications of microparticles include their exploitation as building-blocks for bottom-up tissue engineering strategies, have integrated in vitro 3D cellular tissue/disease models as cue-providers, and have been used as reinforcement units within bioinks for 3D bioprinting.

I.4. Microparticles as cell adhesive and modulating moieties

Over the past few decades, microparticles have gained increasing relevance in tissue engineering and biotechnological strategies. Apart from their mostly widespread application as drug delivery reservoirs with precise local targeting abilities and highly controlled release profiles, a very explored application of microparticles in direct contact with cells is their use as **microcarriers** (see Glossary) for large-scale expansion and differentiation of adherent cells in bioreactors. A plethora of chemical and structural microparticles' formulations has been explored in the search for the most effective and compliant cell expansion strategies, culminating in the exploitation of different types of materials processed with completely different features[1]. The biotechnological value of microcarriers was proven with high yield *in vitro* production of growth factors (GFs) and other soluble molecules, as well as for the rapid expansion of clinically-relevant cells, including stem cells[2,3]. Despite the promising reported outputs, advances in microcarriers design and their optimization to adapt to **xeno-free** scalable and clinically translatable setups, as well as their ability to modulate cell response, are still a growing trend in several segments of biotechnology and biomedical fields[4].

More recent trends have been exploring the potential of micrometric particles beyond the 'carrier' application. They have been successfully used as injectable/fit-to-defect moldable systems proven to form adequate robust 3D structures for *in situ* tissue regeneration[5]. Specialized activities including the ability to selectively recruit different cell types and inducing highly localized responses through the presentation of cell membrane-interacting domains (e.g. GFs) have been important in the advance of vascularization strategies in tissue regeneration, on the fine spatial control over cell differentiation, or on the induction of therapeutic potential[6–9]. The incorporation of biomaterial microparticles into multicellular structures (e.g. **3D spheroids**) has allowed the development of *in vitro* platforms for the generation of complex 3D tissue/disease models, including multicellular tumor models[10–12]. Moreover, the advent of 3D bioprinting brought new insights on possible applications of microparticles as reinforcement units within **bioinks** produced to regenerate injured tissues[13].

With this review, we aim at providing a critical discussion about well-reported particle design factors capable of modulating their (bio)chemical/physical and architectural features (Figure I.1), and how those characteristics correlate with cellular response outputs[7,14]. Novel trends on microparticles design and engineering - including controlled size, geometry, and anisotropy - will also be addressed, as well as their potential on healthcare-related applications. We will discuss microparticles fabrication and highly enabling technologies to produce finely modulated structures with tailored chemical patterns, well-established surface area-to-volume ratios, complex geometries and anisotropy, as well as multicompartmental features.

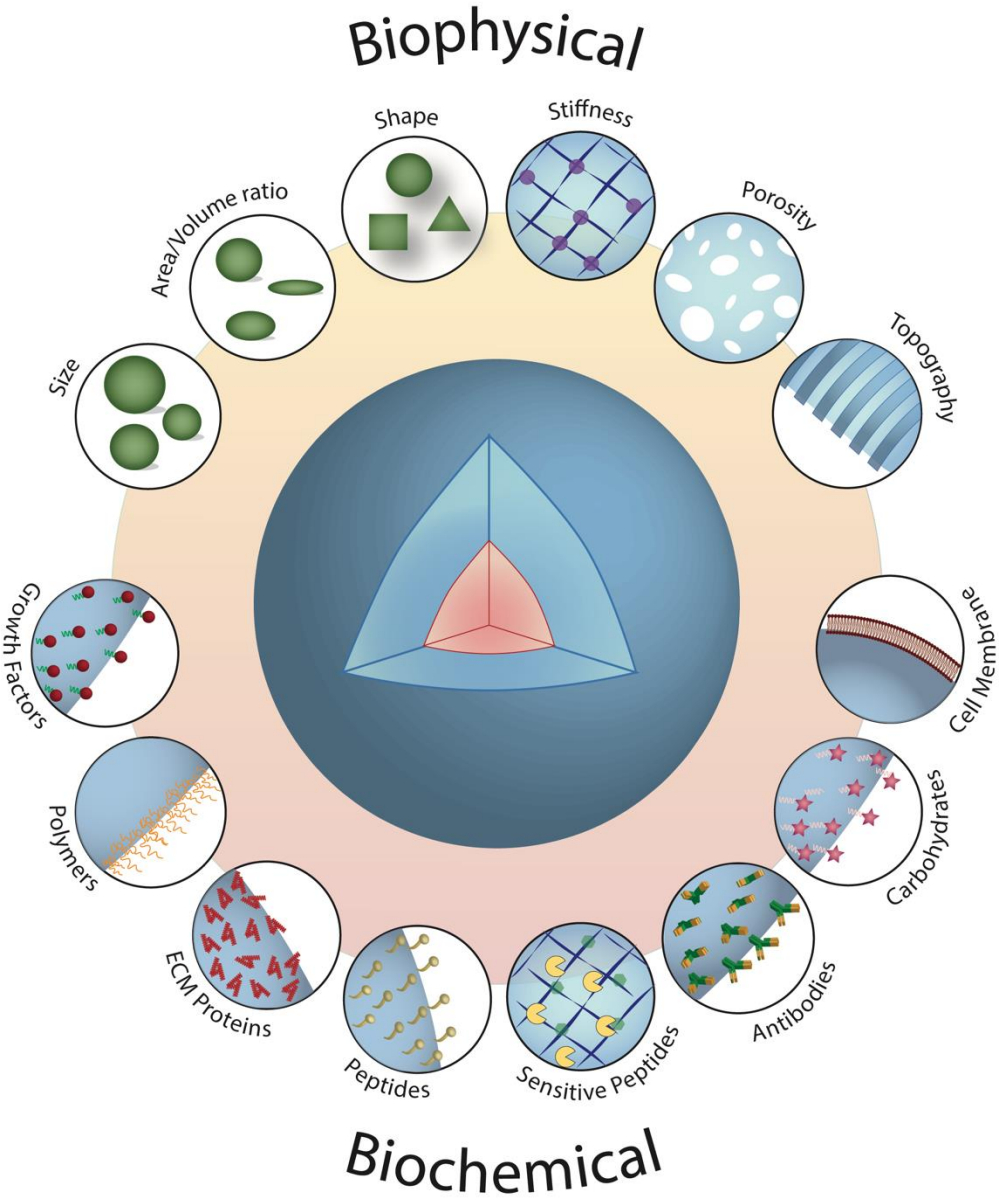

Figure I.1. Schematic representation of (bio)chemical/physical cues and architectural features as modulating moieties of microparticles.

I.5. (Bio)physical and biochemical tailoring of microparticles: applications, needs and technical constrains

I.5.1. Microparticles with controlled (bio)physical aspects

It has long been known that biomaterial properties can affect and modulate several biological outputs[15]. By merely tuning physical properties of the particles such as size,

geometry, anisotropy, topography, stiffness, porosity and compartmentalization, it is plausible to achieve specific biological responses (Table I.1 (page 24-32)) [16–18]. However, the fabrication of microparticles with such desired and controllable physical attributes through conventional methods, namely through emulsion polymerization, still remains a challenge. To overcome these difficulties, various methods were developed in the search of a processes capable of rendering versatile particle with tuneable surface features and morphologies. Microsphere reshaping comprises a simple and scalable method to produce anisotropic complex-shaped particles based on the distortion of microspheres through film-stretching[19] or moulding techniques[20]. This technique uses spheres as the starting material and comprises two main steps: (i) liquefaction, where they are exposed to solvents/vapours or temperatures above polymers' glass-transition temperature and deformed until a desired shape is achieved, and (ii) solidification by extracting the solvent/vapours or by cooling the temperature of the system. Besides being an easy and versatile method, this method may induce damage to the properties and microstructure of the starting material through the exposure to aggressive solvents, which might affect biological activity. Enhancing the gentleness of the procedure can be achieved by using only the vapours of organic solvents, instead of the liquid form[20]. Electrohydrodynamic (EHD) co-jetting is another technique that exhibits great control over particles' anisotropy, size and shape[21]. Similarly to electrospinning, the application of an electric potential results in the stretching of a pendant droplet – the Taylor cone – allowing the formation of well-defined particles with great control over anisotropy, size and geometry, through rapid solvent evaporation. This technique often renders fibers and spheres, but control over several process parameters, such as flow rate and polymer concentration, enables the fabrication of disk- and rod-shaped particles. One particular feature of EDH co-jetting is the ability to produce chemically distinct and **multi-compartmentalized particles** which can be advantageous for controlled drug delivery or cell targeting[22]. Moreover, this technique is compatible with both aqueous and organic solvents, enabling the processing of tailored particles using a wide range of polymers. Alternatively, microfluidics is a versatile method to obtain intricate particle designs with high precision. Besides being suitable for cell encapsulation with tuneable sizes and shapes[23], compartmentalized particles are also easy to attain. Structures with core-shell and multi-core organization, Janus and ternary set-ups[24], internal anisotropic features[25] have been obtained via microfluidics. Tailored porous structures were also achieved through insertion of porogens, such as fine oil droplets, or even through phase inversion[26].

Microparticles are often synthesized using difficult to remove oils, and seldom applied UV-polymerization strategies may be hazardous for biological applications and even to sensitive materials. Highly multifaceted structures may also be processed through microfabrication by the application of different techniques such as photolithography and soft lithography, using photomasks or elastomeric stamps/moulds, respectively[27]. These complex microarchitectures with high resolution have been assembled to fabricate fillable core-shell particles, providing a viable platform for a pulsatile and continuous release of soluble molecules[28]. More recently, the use of bioinspired and biomimetic platforms, namely superhydrophobic (SH) and superamphiphobic (SA) surfaces based on the high repellence of water and/or low-surface-tension liquids ('oils'), has driven the formation of liquid droplets with perfect spherical shape[29]. Inspired by such unique properties a new and cost-effective tool to produce engineered polymeric microspheres and **capsules** using mild conditions was created, allowing the fabrication of hierarchical systems[30]. To suppress the need of multiple pipetting or complex machinery and to allow the fabrication of non-spherical hydrogel particles, a droplet microarray platform combining SH or SA properties was developed[31]. This technique enabled the patterning and retrieval of microparticles with several different geometrical structures, including hexagons, triangles and even heart-shaped particles. Despite the multiple platforms and methods to produce particles with highly intricate and sophisticated structures, there is still a great need of a versatile system to enable the control and tuning of physical properties with high precision and resolution.

I.5.2. Microparticles with controlled biochemical cues

The control over cellular behaviour is dictated not only by the aforementioned physical aspects of the material, but also by (bio)chemical interactions (Table I.1 (pages 24-32)). Strategies based on the presentation of chemical domains to cells through microparticles often comprise the precise and a spatiotemporal delivery of soluble factors to achieve specific paracrine effects through soluble signalling[6,32]. The bulk of the microparticles can be used to encapsulate factors that may be diffused to the surface and be available to control cellular mechanisms[33]. However, the presentation of **tethered** biomolecules is found to improve the ability to direct and modulate cellular response by usually mimicking key components present in native tissues[34]. The most common practice is the immobilization of full-length extracellular matrix (ECM)-derived proteins,

such as laminin and fibronectin, onto microparticles' surface aiming at cell matrix signalling replication and therefore, promoting cell adhesion[35]. Apart from mediating cell attachment and proliferation, these bioactive molecules can also provide signals that trigger cell aggregation and modulate cellular migratory behaviours depending on the selected coating[36,37]. Another ECM-mimicking strategy is the use of decellularized tissue which can better recapitulate the innate microenvironment while providing a native-like and tissue-specific milieu[38]. Besides recreating cell-ECM contacts, it also has been developed systems that mimic cell-cell signalling with adsorption of cellular adhesion molecules (CAMs), namely E-cadherin fusion protein[39]. Being a key regulator of intrinsic cell-cell interactions, it is capable of mediating growth-promoting cell signalling pathways, promoting cell self-renewal, and improving induction or maintenance of stem cell multipotency. To simplify the workload bared by using full-length proteins, the use of biological motifs became widely popular for their relative ease of availability and lower cost of preparation[40]. Among other short peptides of interest, the cell adhesion properties of the RGD peptide (arginylglycylaspartic acid) have been intensely exploited in material functionalization. Present in fibronectin is also found in other ECM proteins such as laminin and vitronectin, has the ability to retain its cell-binding properties and to be recognized by several cell surface integrins, enhancing cellular adhesion[41,42]. Antibodies are another protein family of vast interest in tailoring the surface of microparticles due to their ligand binding specificity and their ability to improve cell adhesion. It provides microparticles with additional and specialized activities, allowing a selectively recruit of different cell types and/or bioactive molecules[8]. This not only allows a better control over cellular function but also provides a feasible platform for specific cell isolation and capture from complex mixtures[9]. Likewise, immobilization of GFs has been a promising approach for providing cues in a well-controlled mode, overcoming limited efficacy shown by diffusional problems of soluble factors while inducing localized effects. For instance, immobilization of vascular endothelial growth factor (VEGF) proved to be a pro-survival agent for cell-based therapies[43] and tethered basic fibroblast growth factor (bFGF) and transforming growth factor β1 (TGF-β1) enhanced cell attachment and proliferation, and also stimulated locally chondrogenesis[44]. Moreover, coating of particles with a specific cell membrane is gaining attention, creating a cell-mimicking microparticle which emulates cell function. Acting as 'synthetic cells', they have the ability to recapitulate biointerfacing activities of the natural cells[45,46]. Surface functionalization with other cues such as **bioinstructive** polymers have also been

employed to modulate cellular responses and recreate a more native environment. Hyaluronic acid (HA) and poly-L-lysine (PLL) microparticles assembled through Layer-by-Layer (LbL) deposition was recently shown to increase cell-anchoring hotspots while simulating an ECM-like environment for the cells[11]. In addition to the different surface coating possibilities, the functionalization method is another key cell behaviour modulator. Stable covalent modifications have provided a stronger support for cells, leading to better cell attachment and spreading, while week and less stable coatings, as of those of surface adsorbed molecules, promoted a more efficient cell release and are more sensible towards cell migration[37]. Although surface modification through immobilization of various cues allows a fine-tuning over material bioactivity, many biological processes and mechanisms in which such decorative moieties play an important role are yet to unravel. Such know-how may help understanding how cell behaviour can be affected and what are the molecular mediators of such process.

I.6. Multidisciplinary Microparticles: translating processing know-how into useful applications

I.6.1. Microcarriers for the ex vivo *expansion of primary cells and stem cells*

As tissue regeneration approaches keep growing at a fast pace, cell-based therapies demand large quantity and high-quality cell numbers. In fact, it is estimated the need of millions to billions of cells per patient for the treatment of a disease. This is a result of the low cell retention in the defect area and also the significant shortage of cells in cell banks. Therefore, the development of an optimized cellular biomanufacture procedure to generate clinically-relevant cell numbers is in demand. A variety of methods for the large expansion of cells have been described, and the multi-tray system in culture flasks, also known as "**cell stacks**", is the most prevailing method. Adopting a scale-out, rather than a scale-up approach, requires a substantially amount of space and manual labour. To bypass such hurdles, microcarriers have been progressively replacing the conventional two-dimensional (2D) flat approach, and were found to outstand the performance of other expansion technologies[47]. In fact, not only achieved cell densities are significantly higher, boosting cellular yields in the overall process, as morphological aspects and mechanosensing properties of the cells can also be modulated by the

surrounding environment, inducing changes in both cytoskeleton and nuclear dispositions, and altering cytokine production rate and expression levels of specific cell markers. Over the years, microcarrier culture within bioreactors have proved to be an easily scalable support for expansion of both primary and stem cells (Figure I.2a)[2,48]. Their highly enhanced surface area enables an increase in cellular yields in a clinically-relevant time-frame, leading to an **off-the-shelf** approach to be used "**on-demand**". Moreover, the combination of process automation, control and monitoring leads to a more robust and cost-effective technology, replacing laborious and poorly controlled processes[49,50]. Consequently, a plethora of microcarriers with different physicochemical properties have been developed and commercialized in the search for the most effective and compliant cell expansion strategy (Table I.2 (pages 33-36)). Regardless of being a very promising approach, microcarriers are often employed in dynamic conditions which promotes hydrodynamic shear stress to the cells. Engineering of either hollow and highly-porous particles provide shelter and allow in-growth of shear-sensitive cells, while only the latter offers a larger culturing surface due to the skeletal structure with highly-interconnected pores, supporting cell attachment and promoting multidirectional cell-cell interactions[1,5,51,52]. However, the traditional concept of the microcarrier as, solely, an expansion technology is becoming obsolete. This system can not only integrate a cell differentiation approach or even act as a transfection agent together with expansion, but also serve as cell delivery vehicles and as modular building-blocks for tissue regeneration (Box 1)[53–55]. Towards these approaches, different materials showcasing features as biodegradability and suitability for implantation were exploited. Those have been processed with different features in order to adapt to the selected application, while avoiding the need to harvest cells via enzymatic treatment which comprises one of the biggest liabilities of microcarrier culture[1,51,56]. Recently, the pursuit of an optimized xeno-free approach has gained momentum, promoting a facilitated translation to clinic setups for *in vivo* applications. Therefore, many strategies have been explored to develop xeno-free microcarriers using ECM-inspired synthetic coatings, such as vitronectin, albumin and laminin, avoiding the need of animal-derived components[50,57–59]. However, xeno-free carriers go beyond the synthetic ECM-based approach. The use of synthetic hydrogels (e.g. polyethylene glycol (PEG)) can offer a viable platform to engineer custom-made particles with the desired mechanical and degradability properties[4]. To this extent, various efforts have been taken to improve and upgrade this culture system beyond its well-established and traditional application as an expansion technology leading to a more

wide-ranging and translatable setup suitable for *in vivo* regeneration.

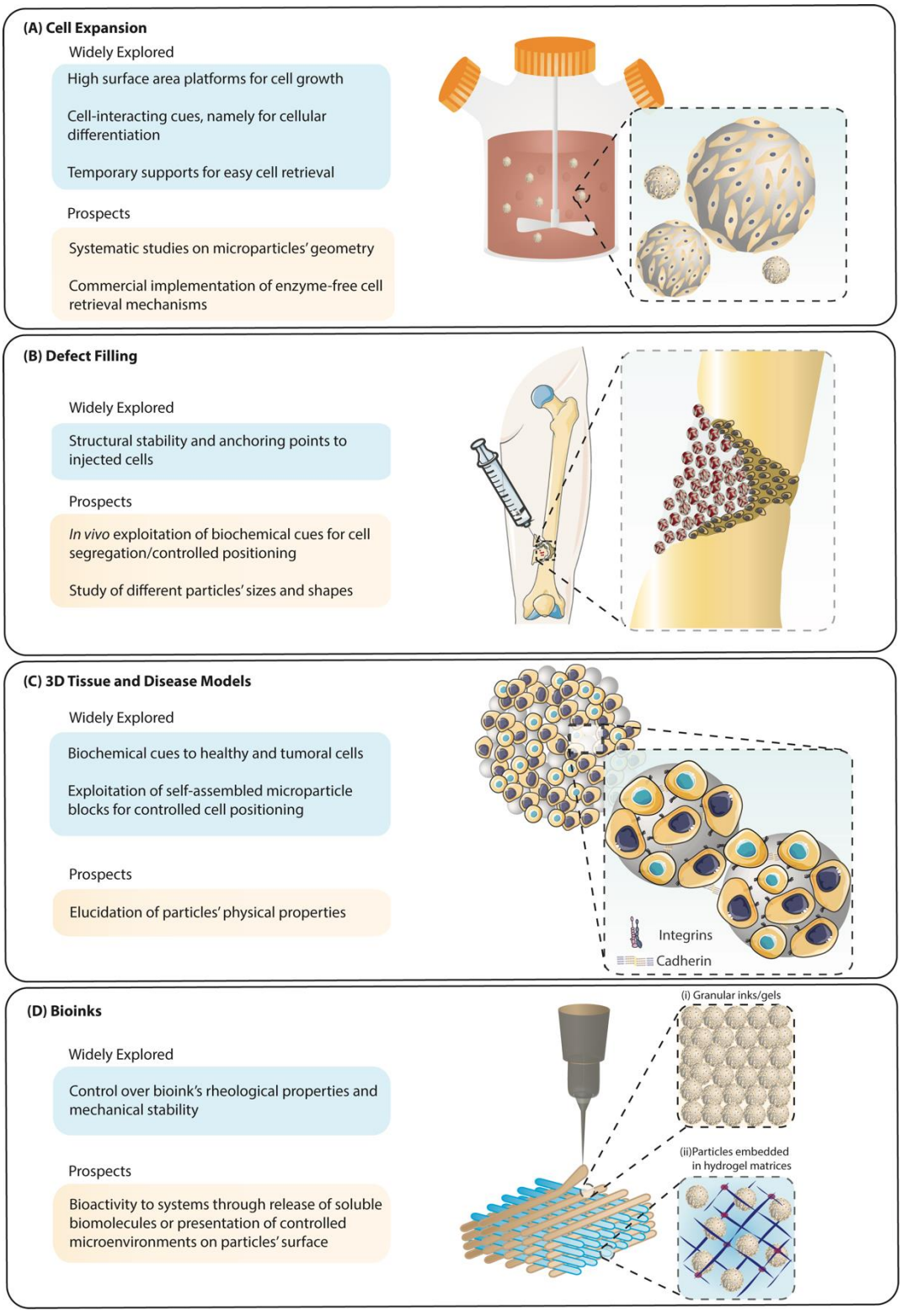

Figure I.2. Overview of the multidisciplinary nature of microparticles. (a) Microparticle conventional approach as microcarrier platforms within bioreactors for large-scale cell expansion and differentiation. **(b)** Microparticles as moldable and

injectable systems, able to accurately fill and fit in irregularly-shaped defects and promote tissue regeneration. **(c)** Microparticles as structural supports and cue providers within multicellular aggregates. **(d)** New generation of modular bioinks composed of **(i)** solely and tightly-packed microparticles (granular inks/gels) and **(ii)** of particle embedded in hydrogel matrices.

Box 1. From modular building-blocks to 3D macroscopic tissue architectures.

Native tissues are characterized by being very intricate systems composed of different cell types conducting a specific function and arranged in a highly ordered structure with a distinct and defined spatial distribution. From a bottom-up tissue engineering strategy perspective, micrometric sized particles, specially, cell-laden particles, reveal a great potential to be used as modular building-blocks to recreate complex tissue functionalities via development of hierarchical and biologically-functional structures[99]. To this extent, several biofabrication techniques such as bioprinting and bioassembly have been explored to engineer organomimetic cellular constructs[100–102]. The automated assembly of the micromodule units is generated through cell-driven organization, by material-material assembly, or hybrid cell-material interactions, usually applied as an injectable platform in a microfabricated mould. Cellular-driven assembly can be accomplished by cell-coated particles, as previously demonstrated by Matsunaga and colleagues, where cells were seeded over collagen particles and injected into a designed mould, promoting cell-cell adhesions[103]. Additionally, cells could migrate and grow within the scaffolding material. This approach expands the potential of these repeating units allowing the development of a more realistic and dynamic microenvironment through co-culture techniques, allowing encapsulation and seeding of different cell types aiming the formation of vascularized tissues. Microparticle annealing, on the other hand, allows the fabrication of a covalently-linked 3D scaffold with interconnected networks of pores suitable for cell migration and integration with the surrounding tissue[41,104]. Providing sufficient space for the cells to expand and proliferate through the construct, this novel biomaterial can circumvent the need of material degradation before neotissue growth. Another particle-driven assembly strategy is based on the direct assembly of, so called, lockyballs, specifically designed to have hoops and loops to enhance random interlocking between neighbouring particles, promoting different levels of flexibility and mobility of the resulting structure[67]. Due to being a hollow structure and having a very porous wall,

these microscaffolds allow an efficient cellularization which allied to the singular architectural features allows a rapid *in situ* tissue construct biofabrication. Although the assembly of macrotissues is often made in a randomly-packed manner, the precision and control over the organization of the building-blocks to produce highly-ordered structures is of great importance in order to recreate accurate tissue-like constructs with physiological significance, such as the anisotropy existent in several tissues and organs[42,105]. These exceedingly precise architectures can be magnetically-driven, through microfluidics and molecular recognition[106,107]. Moreover, a guidance procedure with a clear-cut precision was developed by Yang and co-workers with the ability to manipulate the modules almost in a Lego-like manner into very sophisticated 3D designs[108]. This Tetris-style assembly reveals the undoubtable impact that geometrically designed microstructures may have in the assembly of functional biological structures with complex hierarchical and highly spatially-organized features, closely resembling architectural aspects of the native tissues found within the human body.

I.6.2. Microparticles as building-blocks for tissue engineering and regeneration

Promising applications of microparticles have been reported for their use in the construction of *in vitro* tissue engineering models targeting drug screening and organ-on-a-chip platforms[60], as well as for *in situ* tissue regeneration as an 'one-fits-all' platform to minimize vastly invasive surgical interventions[5]. In fact, the need of an injectable/fit-to-defect moldable scaffold designed to accurately fill any defect site regardless of its shape is of the utmost importance, due to the complexity required to repair any irregularly shaped deformity (Figure I.2b). Despite virtually being the simplest to administrate, 'bulk' hydrogel-based injectable systems can often fail to provide sufficient mechanical stability and durability to support anchorage-dependent cell proliferation and differentiation before the neotissue formation. The application of biodegradable and biocompatible cell-laden microparticles as modular building-blocks could be a suitable and viable way to overcome such limitations[61,62]. For instance, a highly open porous particle with proper surface pores and interconnected passages which protected cells against stress during injection proved to be a viable method to host cell growth and to carry/deliver them to target sites[63]. Moreover, hydrogel-based systems often require prolonged periods of irradiation or the presence of toxic chemical cross-linkers for the *in*

situ gel formation which can be damaging for cell survival. One of the employed strategies to surpass such obstacles comprises the use of particles with inducing gel formation properties where porous and biodegradable microparticles are used as cross-linker carriers to allow *in situ* hydrogel formation under physiological conditions[64]. Another approach was demonstrated by Yu and co-workers who fabricated chitosan microparticles as modular components for tissue engineering, with an ECM-like nanofibrous structure using a physical gelation process without resorting to any toxic or denaturizing agent[65]. Besides acting as cell-anchoring and delivery platforms, these particles can integrate specialized activities such as the ability to selectively recruit different cell types through presentation of bioinstructive moieties (e.g. antibodies and GFs) aiming a better control of cellular function[8,9]. Furthermore, they can also induce highly localized responses, modulating the surrounding microenvironment, acting as life-like 'synthetic cells' capable of communicating with their counterparts and induce biological functions, such as protein production[66] and even emulate stem cell function during tissue repair[45]. Self-assembly of multicellular aggregates with incorporated microparticles can establish interconnected networks and can lead to the formation of robust macroscopic tissue constructs with mechanical stability. For instance, gelatin microspheres were incorporated within self-assembled vascular tissue rings as GFs delivery vehicle and to improve its mechanical properties and morphology[6]. This potentiates the spatially control release of bioactive molecules to help overcome diffusion limitations and allows control of tissue structure and function in order to fabricate more intricate constructs, aiming at novel vascularization strategies. Nonetheless, the assembly process of these building units is not only achieved by cell-driven organization and ECM deposition. In fact, the material itself can be designed in order to improve interlocking ability between contiguous particles, enabling a rapid *in situ* tissue biofabrication[67]. Microparticles have proven to be a suitable approach for the bottom-up engineering of complex 3D constructs and as a plausible injectable system for the *in vivo* regeneration of several tissues such as cartilage[5,14,64,68], bone[63,69–71] and heart[45,72,73]. However, a few drawbacks are yet to overcome regarding implantation within the body. As the structure of the engineered construct might not be perfectly uniform, those can be prone to clogging and cause a blockage in the needle, causing cells to be exposed to a stressful environment due to shear stress that happens during extrusion, culminating in a decrease of cell viability. Once in the body, the particles may exhibit low retention and fixation in the defect area, and may diffuse to other sites, prompting inflammation and embolization, or

impeding the particles' from contacting the surrounding tissue and performing their pro-regenerative role[64]. The scaffolding material and the control over its degradation rate are two critical aspects that may help decrease such problems.

I.6.3. Incorporating microparticles in in vitro *3D Tissues and Disease Models*

The generation of tissue-like constructs or organotypic structures is a fast-growing field, remarkable for therapeutic effects on Regenerative Medicine, with the aim to regenerate or replace tissues and organs[6]. Moreover, these structures are also relevant for research purposes in areas that include cell biology - used to understand underlying cell mechanisms -, and in drug-screening as platforms for toxicity assessment[35,74]. Nowadays, 3D cell culture methods which typically comprises the generation of scaffold-free spheroids cellular aggregates are promising strategies to replace well-established 2D cell culture approaches. Although they can better replicate the physiological tissues' microenvironments in a spatially relevant manner, there are still some limitations that may be surpassed by introducing biomaterials, including micrometric particles, into the cellular constructs[11,75,76]. A common limitation of cell-exclusive aggregates is associated with the lack of vascularization, which limits the transportation and diffusion of nutrients, oxygen or even drugs compared to a vascularized native tissue. Additionally, engineered extracellular environments can fail to reproduce intrinsic signalling cues and the complex organization of the native tissue. Introducing microparticles within the cellular aggregates constitutes a viable way to modulate the biochemical and physical properties of the microenvironment (Figure I.2c). In fact, they can act as reservoirs, providing local and controlled presentation of soluble and tethered molecules. Apart from providing the typical structural support for cell growth[77], they can be loaded with small molecules or present tethered proteins in a precisely-controlled spatiotemporal and uniform manner [78]. This approach proves to be more efficient for morphogen delivery than the simple soluble delivery and it aids directly the differentiation of stem cells. The presentation of cell adhesion molecules also represents a plausible way to direct cell fate and enhance biological functions, due to activation of several signalling pathways[79,80]. The presentation of differentiating moieties is imperative to drive cell lineage commitment, and naïve biomaterials have proven to also influence cellular fate throughout aggregates[81]. Moreover, they can better control aggregate structure, improving its

mechanical properties[82]. These mechanically-tailored particles can modulate cytoskeletal organization and subsequently alter intracellular mechanotransduction signalling cascades[83]. Furthermore, they can also act like sensors, reporting key characteristics of the local microenvironment, such as oxygen and pH levels or even protease activity[84,85]. To this extent, can offer a great way for scale-up approaches and **High-Throughput Screening** (HTS) platforms.

Besides the modelling of healthy tissues[77], there is also the generation of several *in vitro* disease models[10–12,86]. Soker and colleagues demonstrated the creation of a liver-tumor hybrid organoid for tumor growth and as a metastasis model[10]. The use of a microgravity simulating Rotating Wall Vessel (RWV) bioreactor allied to cell culture onto HA and gelatin-coated microcarriers allowed the generation of 3D aggregates based on natural affinities resembling the physiological environment. The hydrogel-coated particles provided a scaffolding surface for cell growth while mimicking the naturally occurring ECM components, facilitating the suspended culture of adherent cells within the bioreactor and promoting an enzyme-free cell release through hydrogel degradability under mildly reductive conditions. In fact, expression of cell surface markers showed significant differences between 2D and 3D culture setups, where in the latter they were consistent with a metastatic phenotype, suggesting its higher relevance as accurate systems to create organotypic structures. Scaffold-free models often lack ECM-like cues and, therefore, there is a deficiency of pre-existing ECM components within the cell aggregate which prevents early ECM deposition, only to be cell-assembled during culture periods, weakening the physical resistance. The incorporation of ECM-mimetics and spatial interconnectivity providers, namely instructive microparticles as cue providers to achieve on-demand biological responses, may improve the ability of the aggregates to better resemble the native physiology while affecting the synthesis of endogenous ECM, already at an early stage of the assembled constructs[12]. Such approach was also applied to engineer hybrid 3D *in vitro* lung tumour model with a robust architecture and an emulating tumour microenvironment which was possible through the incorporation of HA-coated microparticles[11].

I.6.4. Engineering microscaffold-based inks for 3D Bioprinting

3D Bioprinting is a promising biomanufacturing strategy that enables the fabrication of tissue-like constructs with custom-made architectures by the controlled

deposition of a 'raw material' – bioink. However, since it is a relatively new technique there are still some challenges that need to be addressed. Besides the integration of a vascularized network within the constructs, another major challenge is to create functional and clinically-relevant grafts which requires the encapsulation of high amounts of cells[87,88]. Although hydrogels constitute the most desirable material type used for bioink manufacture, they are known for mostly providing highly hydrophilic and bio-inert microenvironments in which suspended cells are constrained to a round shape, regardless of cell type or native morphology that often result in cell depletion and low viability. Moreover, cell-encapsulation strategies in hydrogels are associated with cell constraints and fewer cell interactions due to inadequacy of cell spread and migration. Providing an anchor to support cell growth and proliferation has been suggested as a viable way to conquer this problem. A composite material comprising collagen microcarriers embedded in an alginate hydrogel containing collagenase provided not only a cell-affinitive interface but also sufficient cell spreading spaces upon collagen degradation[89]. Apart from these, most hydrogels are often portrayed as "soft" materials, lacking good mechanical properties for a proper bioprintability. While a hydrogel-based bioink can easily lose its structural integrity, a hybrid microscaffold-based ink, composed by cell-laden microspheres encapsulated in a thin agarose-collagen hydrogel layer, was developed to improve material stability during and post-print. The hydrogel acting as a glue to tightly pack the particles allowed a great improvement of the compression strength compared to the scaffold-free hydrogel[90]. Inspired by the structural stability triggered by the capillary bridges found amid the wetted sand granules in sandcastle formation, Velev and colleagues developed an elastomeric ink composed of polydimethylsiloxane (PDMS) in the form of both precured beads coated with the uncured precursor liquid, which acts as a binding agent[91]. This capillary-based suspension ink renders extremely resilient, but delicate fibres with an excellent elasticity, and flexibility, and controlled porosity, holding a great potential in many biomedical applications. Burdick and colleagues also developed a granular bioink composed exclusively of densely-packed microgels[92]. In this work, cross-linked particles of various types of materials were extruded as stable filaments, either over a surface or within a hydrogel matrix, forming smooth aggregates without interparticle linkages, or even the need of any material as a binding agent. Systems such as injectable cell-laden microcarriers embedded in hydrogels (Figure I.2d) have proven to not only provide platforms for cellular focal adhesion but also facilitate the cells to overcome gel enlacement and fully spread out into their natural morphology, maximizing

cell-cell interactions while providing a structural support throughout the hydrogels' matrices[93]. In fact, a work from Mateos-Timoneda and colleagues shows the fabrication of living osteochondral constructs through bioprinting of mesenchymal stem cell (MSC)-laden polylactic acid (PLA) microcarriers encapsulated in gelatin methacrylamide-gellan gum bioinks[13]. It was demonstrated that PLA microcarriers not only allowed for highly cell-concentrated and viable structures but also improved bioink's compressive modulus, acting as reinforcement units that increase the mechanical strength of the gel without compromising the of the hydrogel network and its bioprintability. Furthermore, this system offered a high cell-anchoring surface that supported osteogenic differentiation and bone matrix deposition compared to cells suspended in the hydrogel system. In addition to these microcarrier/hydrogel hybrid bioinks, different types of materials can be exploited as the extruded material, replacing hydrogel-based inks. Considered as a "soft" material, the mechanical properties of hydrogels do not resemble those exhibited by hard tissues, such as bone. Müller an co-workers fabricated a biomechanically stable bioink with morphogenetic potential, suitable as a bone implant, composed by calcium polyphosphate (Ca-polyP) particles within a poly-ε-caprolactone (PCL) matrix[94]. PolyP promoted bone remodeling and regeneration, as PCL act as a reinforcing material, hardening the scaffold to match that of the bone. Recently, bioprinting devices have been adapted and included in an automated bioassembly system allowing the generation of living constructs, suitable for clinical translation. A multistep bottom-up strategy that combined the fabrication of a layer-by-layer built scaffold and the co-assembly of cell-laden particles within the scaffold enabled the creation of complex hierarchical structures[95]. These evidences reveal the great potential held by microparticle incorporation within printable matrices through 3D bioprinting technology for the fabrication of biomedical models, although some improvements, encompassing nozzle clogging and possible toxic byproducts, are yet to be tackled[96].

I.7. Outstanding Question Box

- What are the most relevant parameters to be considered in particle design for a given application?
- How can microparticles with highly specific and independent physical and/or chemical cues be obtained using scalable methods?

- What is the best particle-to-cell ratio to be used in 3D cellular aggregates to control and promote different phenomena as cell differentiation, increase of mechanical stability, mimetics of the native ECM, or resistance to drugs?
- How can high surface area, xeno-free microcarriers with easy and efficient cell detachment mechanisms and large shelf life be attained?

I.8. Concluding Remarks and Future Perspectives

Microparticles are a multidisciplinary system that find application beyond the traditional delivery of drugs and other soluble molecules. Microcarriers with enhanced surface area proved their biotechnological value as an "off-the-shelf" approach for a rapid and efficient expansion and differentiation of countless clinically-relevant cells while their translation to the clinic remains a stumbling-block. Further research is expected to enable the design of advanced microparticles that showcase features, such as biodegradability, xeno-free set-ups and suitability for implantation to adapt to different applications (see Outstanding Questions Box). Several enabling technologies were explored to modulate microparticles' physical and biochemical aspects and dictate several biological outputs. Still, standardized procedures that enable a precise correlation between material cues and their biological response are in great need to enlighten underlying mechanisms and predictable outputs. Microparticles with such desired features can easily find wider applications in many different fields, namely in bottom-up tissue engineering strategies as modular building-blocks to produce highly intricate 3D tissue constructs with great biological value, but also in 3D tissue and disease models as cue-providers to emulate the native environment, and in 3D bioprinting as reinforcement units of bioinks. Exciting novel trends comprise the use of completely synthetic polymeric hollow particles as life-like artificial cells capable of communicating with their counterparts and induce biological functions as protein production. The role of microparticles in synthetic biology is still to explore and may bring outstanding breakthroughs in the development of completely autonomous or hybrid artificial biological systems.

Table 1. Interplay of microparticle (bio)physical and biochemical cues in cellular response driven by cell attachment to biomaterials.

Type of cue	Material/Moieties	Technique	Biological Response	Application	Ref
(Bio)Physical					
Size	Alginate	Aerodynamically-assisted jetting	Cell attachment and proliferation; Increase of microgel diameter led to a decrease of cellular growth; Cell differentiation exhibited no significant dependence on microgel diameter	Large-scale cell expansion	[97]
Geometry	-	-	-	-	Not Found[#]
Anisotropy	Poly-ε-caprolactone (PCL) with a distinct rough and a smooth	Micromoulding	Strong affinity to fibroblast over hepatocytes;	Cell isolation and protein retrieving from a heterogeneous population	[17]

	surface on the opposite side		The rough side absorbed large amount of proteins which enhanced cell-attractiveness, regardless of cell type; Regulation of cell-adhesion and cell cycle-related genes		
Surface Topography	Polyethylene glycol diacrylate (PEG-DA) with wrinkled surface	Stop-flow lithography	Improved cell attachment and proliferation	Cell microcarriers; Cell physiological studies; Tissue engineering	[18]
Porosity	Polyhydroxyalkanoate (PHA)	G/O/W emulsion assisted with releases of carbon dioxide and ammonium bicarbonate degradation	High *in vitro* cell adhesion, continuous proliferation and improved differentiation of hMSCs;	Enhanced surface area cell carrier; Cell ingrowth and protection from shear stress;	[63]

			Supported osteoblast regeneration	Tissue engineering as an injectable cell delivery system	
	Chitosan	W/O emulsion-based thermally induce phase separation	Improved cell attachment, growth and spreading throughout the porous structure; Enhanced cellular activity and functions	Microcarriers for high-performance 3D cell culture	[1]
Compartmentalization	Various biodegradable polymers and a pH-responsive polymer.	Phase separation in microfluidics	-	Cell microcarriers; Selectively release therapeutic agents at acidic environments	[24]
Stiffness	Polydimethylsiloxane (PDMS) with three different elastic moduli (soft, intermediate, stiff)	Curing of O/W emulsion non-crosslinked microdroplets;	Cell attachment and proliferation;	Engineering toolkit for multicellular organoids in disease modelling and tissue engineering applications	[83]

		Different stiffness is attained adjusting the PDMS-curing agent ratio	Soft and stiff particles guided towards osteogenesis; Intermediate stiffness induced chondrogenesis, similarly to particle-free spheroids		
Biochemical					
Antibody immobilization	Chitosan presenting anti-CD31 or anti-CD90	Aerodynamically-assisted jetting for particle fabrication and surface functionalization via Biotin/Streptadivin	Cell attachment and proliferation; Capture of HUVECs by CD31 and ASCs by CD90	Specific cell selection/ isolation from heterotypic cell populations	[9]
Growth factors immobilization	Collagen type I presenting bFGF or TGF-β1	Homogenization in Dispomix Drive system (Axonlab) for particle formation and functionalization via carbodiimide chemistry	Improved cell attachment and proliferation; Local stimulation of cells (chondrogenesis)	Expansion and chondrogenic differentiation	[44]

	Chitosan presenting Platelet Derived Growth Factor-BB (PDGF-BB), TGF-β1 and VEGF	Aerodynamically-assisted jetting for microsphere formation and functionalization via carbodiimide chemistry	Improved cell attachment and proliferation of ASCs	Tissue regeneration as an injectable cell delivery system	[8]
	Polystyrene-coated iron oxide microparticles presenting VEGF	VEGF immobilization via Histidine/Biotin/Streptavidin chemistry	Cell attachment and proliferation; Enhanced survival of outgrowth both in vitro and in vivo	Treatment of ischemic diseases	[43]
Biological motifs	Multi-armed PEG–vinyl sulphone presenting RGD	Microfluidic w/o emulsion for spherical microgel formation	Cell attachment and proliferation; Cell migration and integration in a 3D complex network	Tissue engineering as an injectable cell delivery system	[98]
	PEG-diacrylate (PEG-DA) presenting RGD	Polymer photo-polymerization and functionalization via acryloyl-PEG-RGDS	Improved cell attachment and proliferation	Tissue engineering of 3D vascularized microtissues	[42]

	RGD-coated PLA microcarriers	PLA particles were formed by atomization of the solution into droplets and then precipitated in a coagulation bath; RGD coating was achieved by either covalent modification or physiosorbed	Covalently-linked RGD showed a slight increase in cell adhesion and better cell proliferation capacity compared to the adsorbed coating; Surface adsorbed RGD enhance cell release, promoting a better cell migration ability	Manipulation over cell adhesion and migratory potential of cells	[37]
Cell membrane-coated particles (Cell-mimicking microparticles)	Cellulose decorated with red blood cell membrane	Electrospraying for red blood cell-shaped microparticle formation and coating by sonication	Prolonged circulation time of the microparticles in the blood	Drug delivery	[46]
	PLGA decorated with cardiac stem cell membrane and secretome	W/O/W emulsion and membrane coating by sonication	Cell attachment and proliferation; Emulation of the paracrine and	Therapeutic cardiac regeneration	[45]

				biointerfacing activities of cardiac stem cells		
Proteins	ECM-derived	Laminin- and fibronectin-coated melamine resin microparticles	Proteins were adsorbed to microparticles surface	Increased β-cells adhesion to fibronectin over laminin	Study islet cell biology	[35]
		Pancreatic decellularized matrix-coated PEG-co-PLL	Microfluidic for microspheres synthesis and absorption of decellularized tissue	Improved cell survival, expression of β-cell specific genes and glucose stimulated insulin secretion	Maintenance of β-cell phenotype and function *in vitro* for diabetes therapy	[38]
		Laminin- and vitronectin-coated PS particles with a PLL layer	Both laminin and vitronectin were adsorbed onto the particles	Combining the polyelectrolyte layer with the ECM protein, cell affinity was enhanced; Laminin coating provide a better support for cell attachment and	Generation of a large-scale cell expansion system under continuous agitation	[36]

				aggregation even under continuous agitation; Vitronectin coating requires a static pause to allow cell aggregation		
		Collagen-coated PLA microcarriers	PLA particles were formed by atomization of the solution into droplets and then precipitated in a coagulation bath; Collagen was covalently-linked and adsorbed onto carriers' surface	Covalently-linked collagen promoted a better cell attachment and proliferation; While adsorbed collagen promoted a mild cell attachment to the carrier, having a better cell release profile	Manipulation over cell adhesion and migratory potential of cells	[37]
	Cell adhesion	PLGA decorated with E-cadherin fusion protein	O/W emulsion and solvent evaporation and protein immobilization via surface adsorption	Cell attachment proliferation and cytokine secretion	Cell expansion and controlled delivery of GFs	[39]

	molecules (CAMs)					
Polymers		PLL- and HA-coated PCL microparticles	O/W emulsion and solvent evaporation for PCL particles fabrication; LbL deposition of PLL and HA for surface functionalization	Cell attachment and proliferation Emulation of tumour environment by providing cell-ECM interactions and increased matrix deposition	Tumour-ECM mimetic support; Cell-anchoring hotspots; Study cell response to chemotherapeutics	[11]

[#]Applications only found for cell internalization and drug delivery purposes.

Table 2. Physicochemical properties of commercialized microcarriers.

Microcarrier	Manufacturer	Material	Surface Feature	Shape	Size[#]/Pore size (µm)	Density (g/mL)	Surface Area (cm^2/g)	Storage Conditions	Harvesting method
Positively Charged (protein-free)									
Cytodex 1™	GE Healthcare	Dextran	DEAE	Spherical	147-248/n.a.	1.03	4400	RT	Trypsin
DE-52	Whatman™	Cellulose (biodegradable)	DEAE	Cylindrical	L 130 x D 35 /n.a.	0.9	6800	RT	Trypsin
DE-53	Whatman™	Cellulose (biodegradable)	DEAE	Cylindrical	L 130 x D 35 /n.a.	1.1	6800	RT	Trypsin
QA-52	Whatman™	Cellulose (biodegradable)	Quaternary Ammonium	Cylindrical	L 130 x D 35 /n.a.	1.2	6800	RT	Trypsin
Hillex®	SoloHill	Polystyrene	Cationic Trimethyl Ammonium	Spherical	160-200/n.a.	1.09-1.15	-	RT	Trypsin
Hillex II (HLX II-107)	SoloHill (Thermo Scientific)	Polystyrene	TEA	Spherical	160-180/n.a.	1.12	515	RT	Trypsin
Plastic Plus (P Plus-102-L)	SoloHill (Thermo Scientific)	Polystyrene	Uncoated	Spherical	125-212/n.a.	1.034-1.046	360	RT	Trypsin
FACT III (FACT 102-L)	SoloHill	Polystyrene	Uncoated	Spherical	125-	1.02	360	RT	Trypsin

	(Thermo Scientific)				212/n.a.				
Non/Negatively Charged (protein-free)									
Enhanced Attachment	Corning	Polystyrene	CellBIND Treatment	Spherical	125-212/n.a	1.022-1.030	360	4ªC	Trypsin
Plastic (P 102-L)	SoloHill (Thermo Scientific)	Polystyrene	Uncoated	Spherical	125-212/n.a.	1.02	360	RT	Trypsin
2D MicroHex™	Nunc	Polystyrene	Nunclon™ Treatment	Flat hexagons	L 125 x W 25 /n.a.	1.05	360	RT	Trypsin
SphereCol®	Advanced BioMatrix	Type I Collagen (bovine) (bioegradable)	Uncoated	Spherical	100-400/n.a.	1.022-1.030	-	2-10ºC	Trypsin
G2767	Merck (former Sigma Aldrich)	Glass	Uncoated	Spherical	150-210/n.a.	1.03	-	RT	Trypsin
G2517	Merck (former Sigma Aldrich)	Glass	Uncoated	Spherical	90-150/n.a.	1.03	-	RT	Trypsin
G2892	Merck (former Sigma Aldrich)	Glass	Uncoated	Spherical	90-150/n.a.	1.04	-	RT	Trypsin
Collagen Coated									
Collagen (CGEN 102-L)	SoloHill (Thermo Scientific)	Polystyrene	Type I Collagen (porcine)	Spherical	125-212/n.a.	1.02	480	RT	Trypsin
Cytodex 3™	GE Healthcare	Dextran	Denatured	Spherical	141-	1.04	2700	RT	Trypsin

			Type I Collagen (porcine)		211/n.a.				
ECM Coated									
ProNectin® F (Pro-F 102-L)	SoloHill (Thermo Scientific)	Polystyrene	Recombinant Fibronectin	Spherical	125-212/n.a.	1.02	-	RT	Trypsin
Synthemax® II	Corning	Polystyrene	Synthemax® II	Spherical	125-212/n.a.	1.022-1.030	360	4ºC	Trypsin
Macroporous									
Cultispher-G™	Thermo Scientific	Gelatin (biodegradable)	Uncoated	Spherical	130-380/10-20	1.03	40000	RT	Trypsin
Cultispher-S™	Thermo Scientific	Gelatin (biodegradable)	Uncoated	Spherical	130-380/10-20	1.03	75000	RT	Trypsin
Cultispher-GL™	Thermo Scientific	Gelatin (biodegradable)	Uncoated	Spherical	130-380/50-70	1.03	-	RT	Trypsin
Cytopore 1™	GE Healthcare	Dextran	DEAE	Spherical	200-280/30	1.03	11000	RT	Trypsin
Cytopore 2™	GE Healthcare	Dextran	DEAE	Spherical	200-280/30	1.03	11000	RT	Trypsin
High density									
Cytoline™	GE Healthcare	Polyethylene & Silica	Uncoated	Lens-shaped	L 2100 x W 750 /10-400	1.32	-	RT	Trypsin

Temporary									
Dissolvable Microcarriers	Corning	Polygalacturonic acid crosslinked with calcium ions	Denaturated Type I Collagen (Porcine) or Synthemax® II	Spherical	200-300, fully hydrated	1.02-1.03	5000	RT/4ºC	Bead dissolution by EDTA-chelation of calcium ions, exposing polymer chains to pectinase

Abbreviations: n.a. - not applicable; EDTA – Ethylenediaminetretacetic acid; DEAE - Diethylaminoethyl; TEA - Triethylamine; RT – Room temperature - Data not found

[#]Swelled (When applicable)

I.9. References

1. Huang, L., Xiao, L., Jung Poudel, A., Li, J., Zhou, P., Gauthier, M., Liu, H., Wu, Z. & Yang, G. Porous chitosan microspheres as microcarriers for 3D cell culture. *Carbohydr. Polym.* **202**, 611–620 (2018).
2. Rafiq, Q. A., Hanga, M. P., Heathman, T. R. J., Coopman, K., Nienow, A. W., Williams, D. J. & Hewitt, C. J. Process development of human multipotent stromal cell microcarrier culture using an automated high-throughput microbioreactor. *Biotechnol. Bioeng.* **114**, 2253–2266 (2017).
3. Oliveira, M. B. & Mano, J. F. Polymer-based microparticles in tissue engineering and regenerative medicine. *Biotechnol. Prog.* **27**, 897–912 (2011).
4. Dias, A. D., Elicson, J. M. & Murphy, W. L. Microcarriers with Synthetic Hydrogel Surfaces for Stem Cell Expansion. *Adv. Healthc. Mater.* **6**, 1700072 (2017).
5. Wang, Y., Yuan, X., Yu, K., Meng, H., Zheng, Y., Peng, J., Lu, S., Liu, X., Xie, Y. & Qiao, K. Fabrication of nanofibrous microcarriers mimicking extracellular matrix for functional microtissue formation and cartilage regeneration. *Biomaterials* **171**, 118–132 (2018).
6. Strobel, H. A., Dikina, A. D., Levi, K., Solorio, L. D., Alsberg, E. & Rolle, M. W. Cellular Self-Assembly with Microsphere Incorporation for Growth Factor Delivery Within Engineered Vascular Tissue Rings. *Tissue Eng. Part A* **23**, 143–155 (2017).
7. Le, L. V., Mohindra, P., Fang, Q., Sievers, R. E., Mkrtschjan, M. A., Solis, C., Safranek, C. W., Russell, B., Lee, R. J. & Desai, T. A. Injectable hyaluronic acid based microrods provide local micromechanical and biochemical cues to attenuate cardiac fibrosis after myocardial infarction. *Biomaterials* **169**, 11–21 (2018).
8. Custódio, C. A., Santo, V. E., Oliveira, M. B., Gomes, M. E., Reis, R. L. & Mano, J. F. Functionalized Microparticles Producing Scaffolds in Combination with Cells. *Adv. Funct. Mater.* **24**, 1391–1400 (2014).
9. Custódio, C. A., Cerqueira, M. T., Marques, A. P., Reis, R. L. & Mano, J. F. Cell selective chitosan microparticles as injectable cell carriers for tissue regeneration. *Biomaterials* **43**, 23–31 (2015).
10. Skardal, A., Devarasetty, M., Rodman, C., Atala, A. & Soker, S. Liver-Tumor

Hybrid Organoids for Modeling Tumor Growth and Drug Response In Vitro. *Ann. Biomed. Eng.* **43**, 2361–2373 (2015).

11. Ferreira, L. P., Gaspar, V. M. & Mano, J. F. Bioinstructive microparticles for self-assembly of mesenchymal stem Cell-3D tumor spheroids. *Biomaterials* **185**, 155–173 (2018).
12. Brancato, V., Gioiella, F., Imparato, G., Guarnieri, D., Urciuolo, F. & Netti, P. A. 3D breast cancer microtissue reveals the role of tumor microenvironment on the transport and efficacy of free-doxorubicin in vitro. *Acta Biomater.* **75**, 200–212 (2018).
13. Levato, R., Visser, J., Planell, J. A., Engel, E., Malda, J. & Mateos-Timoneda, M. A. Biofabrication of tissue constructs by 3D bioprinting of cell-laden microcarriers. *Biofabrication* **6**, 035020 (2014).
14. Morille, M., Toupet, K., Montero-Menei, C. N., Jorgensen, C. & Noël, D. PLGA-based microcarriers induce mesenchymal stem cell chondrogenesis and stimulate cartilage repair in osteoarthritis. *Biomaterials* **88**, 60–69 (2016).
15. Mitragotri, S. & Lahann, J. Physical approaches to biomaterial design. *Nat. Mater.* **8**, 15–23 (2009).
16. He, Y. & Park, K. Effects of the Microparticle Shape on Cellular Uptake. *Mol. Pharm.* **13**, 2164–71 (2016).
17. Zheng, H., Du, W., Duan, Y., Geng, K., Deng, J. & Gao, C. Biodegradable Anisotropic Microparticles for Stepwise Cell Adhesion and Preparation of Janus Cell Microparticles. *ACS Appl. Mater. Interfaces* **10**, 36776–36785 (2018).
18. Li, M., Joung, D., Hughes, B., Waldman, S. D., Kozinski, J. A. & Hwang, D. K. Wrinkling Non-Spherical Particles and Its Application in Cell Attachment Promotion. *Sci. Rep.* **6**, 30463 (2016).
19. Meyer, R. A., Meyer, R. S. & Green, J. J. An automated multidimensional thin film stretching device for the generation of anisotropic polymeric micro- and nanoparticles. *J. Biomed. Mater. Res. Part A* **103**, 2747–2757 (2015).
20. de Alteriis, R., Vecchione, R., Attanasio, C., De Gregorio, M., Porzio, M., Battista, E. & Netti, P. A. A method to tune the shape of protein-encapsulated polymeric microspheres. *Sci. Rep.* **5**, 12634 (2015).
21. Bhaskar, S. & Lahann, J. Microstructured Materials Based on Multicompartmental Fibers. *J. Am. Chem. Soc.* **131**, 6650–6651 (2009).
22. Bhaskar, S., Pollock, K. M., Yoshida, M. & Lahann, J. Towards Designer

Microparticles: Simultaneous Control of Anisotropy, Shape, and Size. *Small* **6**, 404–411 (2010).

23. Choi, C.-H., Wang, H., Lee, H., Kim, J. H., Zhang, L., Mao, A., Mooney, D. J. & Weitz, D. A. One-step generation of cell-laden microgels using double emulsion drops with a sacrificial ultra-thin oil shell. *Lab Chip* **16**, 1549–55 (2016).
24. Min, N. G., Ku, M., Yang, J. & Kim, S.-H. Microfluidic Production of Uniform Microcarriers with Multicompartments through Phase Separation in Emulsion Drops. *Chem. Mater.* **28**, 1430–1438 (2016).
25. Qiu, Y., Wang, F., Liu, Y.-M., Wang, W., Chu, L.-Y. & Wang, H.-L. Microfluidic-based fabrication, characterization and magnetic functionalization of microparticles with novel internal anisotropic structure. *Sci. Rep.* **5**, 13060 (2015).
26. Udoh, C. E., Garbin, V. & Cabral, J. T. Microporous Polymer Particles via Phase Inversion in Microfluidics: Impact of Nonsolvent Quality. *Langmuir* **32**, 8131–8140 (2016).
27. Choi, C.-H., Kang, S. M., Jin, S. H., Yi, H. & Lee, C. S. Controlled fabrication of multicompartmental polymeric microparticles by sequential micromolding via surface-tension-induced droplet formation. *Langmuir* **31**, 1328–1335 (2015).
28. McHugh, K. J., Nguyen, T. D., Linehan, A. R., Yang, D., Behrens, A. M., Rose, S., Tochka, Z. L., Tzeng, S. Y., Norman, J. J., Anselmo, A. C., Xu, X., Tomasic, S., Taylor, M. A., Lu, J., Guarecuco, R., Langer, R. & Jaklenec, A. Fabrication of fillable microparticles and other complex 3D microstructures. *Science* **357**, 1138–1142 (2017).
29. Neto, A. I., Levkin, P. A. & Mano, J. F. Patterned superhydrophobic surfaces to process and characterize biomaterials and 3D cell culture. *Mater. Horizons* **5**, 379–393 (2018).
30. Costa, A. M. S. & Mano, J. F. Solvent-Free Strategy Yields Size and Shape-Uniform Capsules. *J. Am. Chem. Soc.* **139**, 1057–1060 (2017).
31. Neto, A. I., Demir, K., Popova, A. A., Oliveira, M. B., Mano, J. F. & Levkin, P. A. Fabrication of Hydrogel Particles of Defined Shapes Using Superhydrophobic-Hydrophilic Micropatterns. *Adv. Mater.* **28**, 7613–7619 (2016).
32. Heidariyan, Z., Ghanian, M. H., Ashjari, M., Farzaneh, Z., Najarasl, M., Rezaei Larijani, M., Piryaei, A., Vosough, M. & Baharvand, H. Efficient and cost-

effective generation of hepatocyte-like cells through microparticle-mediated delivery of growth factors in a 3D culture of human pluripotent stem cells. *Biomaterials* **159**, 174–188 (2018).

33. Martins, C. R., Custódio, C. A. & Mano, J. F. Multifunctional laminarin microparticles for cell adhesion and expansion. *Carbohydr. Polym.* **202**, 91–98 (2018).
34. Custódio, C. A., Reis, R. L. & Mano, J. F. Engineering Biomolecular Microenvironments for Cell Instructive Biomaterials. *Adv. Healthc. Mater.* **3**, 797–810 (2014).
35. Bernard, A. B., Chapman, R. Z. & Anseth, K. S. Controlled local presentation of matrix proteins in microparticle-laden cell aggregates. *Biotechnol. Bioeng.* **111**, 1028–1037 (2014).
36. Lam, A. T.-L., Li, J., Chen, A. K.-L., Reuveny, S., Oh, S. K.-W. & Birch, W. R. Cationic surface charge combined with either vitronectin or laminin dictates the evolution of human embryonic stem cells/microcarrier aggregates and cell growth in agitated cultures. *Stem Cells Dev.* **23**, 1688–703 (2014).
37. Levato, R., Planell, J. A., Mateos-Timoneda, M. A. & Engel, E. Role of ECM/peptide coatings on SDF-1α triggered mesenchymal stromal cell migration from microcarriers for cell therapy. *Acta Biomater.* **18**, 59–67 (2015).
38. Li, W., Lee, S., Ma, M., Kim, S. M., Guye, P., Pancoast, J. R., Anderson, D. G., Weiss, R., Lee, R. T. & Hammond, P. T. Microbead-based biomimetic synthetic neighbors enhance survival and function of rat pancreatic β-cells. *Sci. Rep.* **3**, 2863 (2013).
39. Zhang, Y., Mao, H., Gao, C., Li, S., Shuai, Q., Xu, J., Xu, K., Cao, L., Lang, R., Gu, Z., Akaike, T. & Yang, J. Enhanced Biological Functions of Human Mesenchymal Stem-Cell Aggregates Incorporating E-Cadherin-Modified PLGA Microparticles. *Adv. Healthc. Mater.* **5**, 1949–1959 (2016).
40. Wronska, M. A., O'Connor, I. B., Tilbury, M. A., Srivastava, A. & Wall, J. G. Adding Functions to Biomaterial Surfaces through Protein Incorporation. *Adv. Mater.* **28**, 5485–5508 (2016).
41. Griffin, D. R., Weaver, W. M., Scumpia, P. O., Di Carlo, D. & Segura, T. Accelerated wound healing by injectable microporous gel scaffolds assembled from annealed building blocks. *Nat. Mater.* **14**, 737–744 (2015).
42. Wang, H., Cui, J., Zheng, Z., Shi, Q., Sun, T., Liu, X., Huang, Q. & Fukuda, T.

Assembly of RGD-Modified Hydrogel Micromodules into Permeable Three-Dimensional Hollow Microtissues Mimicking in Vivo Tissue Structures. *ACS Appl. Mater. Interfaces* **9**, 41669–41679 (2017).

43. Aday, S., Zoldan, J., Besnier, M., Carreto, L., Saif, J., Fernandes, R., Santos, T., Bernardino, L., Langer, R., Emanueli, C. & Ferreira, L. Synthetic microparticles conjugated with VEGF165 improve the survival of endothelial progenitor cells via microRNA-17 inhibition. *Nat. Commun.* **8**, 747 (2017).
44. Bertolo, A., Arcolino, F., Capossela, S., Taddei, A. R., Baur, M., Pötzel, T. & Stoyanov, J. Growth Factors Cross-Linked to Collagen Microcarriers Promote Expansion and Chondrogenic Differentiation of Human Mesenchymal Stem Cells. *Tissue Eng. Part A* **21**, 2618–2628 (2015).
45. Tang, J., Shen, D., Caranasos, T. G., Wang, Z., Vandergriff, A. C., Allen, T. A., Hensley, M. T., Dinh, P.-U., Cores, J., Li, T.-S., Zhang, J., Kan, Q. & Cheng, K. Therapeutic microparticles functionalized with biomimetic cardiac stem cell membranes and secretome. *Nat. Commun.* **8**, 13724 (2017).
46. Hayashi, K., Yamada, S., Sakamoto, W., Usugi, E., Watanabe, M. & Yogo, T. Red Blood Cell-Shaped Microparticles with a Red Blood Cell Membrane Demonstrate Prolonged Circulation Time in Blood. *ACS Biomater. Sci. Eng.* **4**, 2729–2732 (2018).
47. Shekaran, A., Sim, E., Tan, K. Y., Chan, J. K. Y., Choolani, M., Reuveny, S. & Oh, S. Enhanced in vitro osteogenic differentiation of human fetal MSCs attached to 3D microcarriers versus harvested from 2D monolayers. *BMC Biotechnol.* **15**, 102 (2015).
48. Gupta, P., Ismadi, M.-Z., Verma, P. J., Fouras, A., Jadhav, S., Bellare, J. & Hourigan, K. Optimization of agitation speed in spinner flask for microcarrier structural integrity and expansion of induced pluripotent stem cells. *Cytotechnology* **68**, 45–59 (2016).
49. Borys, B. S., Roberts, E. L., Le, A. & Kallos, M. S. Scale-up of embryonic stem cell aggregate stirred suspension bioreactor culture enabled by computational fluid dynamics modeling. *Biochem. Eng. J.* **133**, 157–167 (2018).
50. Eicke, D., Baigger, A., Schulze, K., Latham, S. L., Halloin, C., Zweigerdt, R., Guzman, C. A., Blasczyk, R. & Figueiredo, C. Large-scale production of megakaryocytes in microcarrier-supported stirred suspension bioreactors. *Sci. Rep.* **8**, 10146 (2018).

51. Confalonieri, D., La Marca, M., van Dongen, E. M. W. M., Walles, H. & Ehlicke, F. * An Injectable Recombinant Collagen I Peptide-Based Macroporous Microcarrier Allows Superior Expansion of C2C12 and Human Bone Marrow-Derived Mesenchymal Stromal Cells and Supports Deposition of Mineralized Matrix. *Tissue Eng. Part A* **23**, 946–957 (2017).
52. YekrangSafakar, A., Acun, A., Choi, J.-W., Song, E., Zorlutuna, P. & Park, K. Hollow microcarriers for large-scale expansion of anchorage-dependent cells in a stirred bioreactor. *Biotechnol. Bioeng.* **115**, 1717–1728 (2018).
53. Srinivasan, G., Morgan, D., Varun, D., Brookhouser, N. & Brafman, D. A. An integrated biomanufacturing platform for the large-scale expansion and neuronal differentiation of human pluripotent stem cell-derived neural progenitor cells. *Acta Biomater.* **74**, 168–179 (2018).
54. Hsu, C. Y. M., Walsh, T., Borys, B. S., Kallos, M. S. & Rancourt, D. E. An Integrated Approach toward the Biomanufacturing of Engineered Cell Therapy Products in a Stirred-Suspension Bioreactor. *Mol. Ther. - Methods Clin. Dev.* **9**, 376–389 (2018).
55. Martin, Y. H., Jubin, K., Smalley, S., Wong, J. P. F., Brown, R. A. & Metcalfe, A. D. A novel system for expansion and delivery of human keratinocytes for the treatment of severe cutaneous injuries using microcarriers and compressed collagen. *J. Tissue Eng. Regen. Med.* **11**, 3124–3133 (2017).
56. Li, C., Qian, Y., Zhao, S., Yin, Y. & Li, J. Alginate/PEG based microcarriers with cleavable crosslinkage for expansion and non-invasive harvest of human umbilical cord blood mesenchymal stem cells. *Mater. Sci. Eng. C* **64**, 43–53 (2016).
57. Fan, Y., Zhang, F. & Tzanakakis, E. S. Engineering Xeno-Free Microcarriers with Recombinant Vitronectin, Albumin and UV Irradiation for Human Pluripotent Stem Cell Bioprocessing. *ACS Biomater. Sci. Eng.* **3**, 1510–1518 (2017).
58. Rodrigues, C. A., Silva, T. P., Nogueira, D. E., Fernandes, T. G., Hashimura, Y., Wesselschmidt, R., Diogo, M. M., Lee, B. & Cabral, J. M. Scalable culture of human induced pluripotent cells on microcarriers under xeno-free conditions using single-use vertical-wheel™ bioreactors. *J. Chem. Technol. Biotechnol.* **93**, 3597–3606 (2018).
59. Badenes, S. M., Fernandes, T. G., Miranda, C. C., Pusch-Klein, A., Haupt, S.,

Rodrigues, C. A., Diogo, M. M., Brüstle, O. & Cabral, J. M. Long-term expansion of human induced pluripotent stem cells in a microcarrier-based dynamic system. *J. Chem. Technol. Biotechnol.* **92**, 492–503 (2017).

60. Zhang, C., Zhao, Z., Abdul Rahim, N. A., van Noort, D. & Yu, H. Towards a human-on-chip: Culturing multiple cell types on a chip with compartmentalized microenvironments. *Lab Chip* **9**, 3185 (2009).
61. Leferink, A., Schipper, D., Arts, E., Vrij, E., Rivron, N., Karperien, M., Mittmann, K., van Blitterswijk, C., Moroni, L. & Truckenmüller, R. Engineered Micro-Objects as Scaffolding Elements in Cellular Building Blocks for Bottom-Up Tissue Engineering Approaches. *Adv. Mater.* **26**, 2592–2599 (2014).
62. Yajima, Y., Yamada, M., Utoh, R. & Seki, M. Collagen Microparticle-Mediated 3D Cell Organization: A Facile Route to Bottom-up Engineering of Thick and Porous Tissues. *ACS Biomater. Sci. Eng.* **3**, 2144–2154 (2017).
63. Wei, D.-X., Dao, J.-W. & Chen, G.-Q. A Micro-Ark for Cells: Highly Open Porous Polyhydroxyalkanoate Microspheres as Injectable Scaffolds for Tissue Regeneration. *Adv. Mater.* **30**, 1802273 (2018).
64. Liao, J., Wang, B., Huang, Y., Qu, Y., Peng, J. & Qian, Z. Injectable Alginate Hydrogel Cross-Linked by Calcium Gluconate-Loaded Porous Microspheres for Cartilage Tissue Engineering. *ACS Omega* **2**, 443–454 (2017).
65. Zhou, Y., Gao, H.-L., Shen, L.-L., Pan, Z., Mao, L.-B., Wu, T., He, J.-C., Zou, D.-H., Zhang, Z.-Y. & Yu, S.-H. Chitosan microspheres with an extracellular matrix-mimicking nanofibrous structure as cell-carrier building blocks for bottom-up cartilage tissue engineering. *Nanoscale* **8**, 309–317 (2016).
66. Niederholtmeyer, H., Chaggan, C. & Devaraj, N. K. Communication and quorum sensing in non-living mimics of eukaryotic cells. *Nat. Commun.* **9**, 5027 (2018).
67. Silva, K. R., Rezende, R. A., Pereira, F. D. A. S., Gruber, P., Stuart, M. P., Ovsianikov, A., Brakke, K., Kasyanov, V., da Silva, J. V. L., Granjeiro, J. M., Baptista, L. S. & Mironov, V. Delivery of Human Adipose Stem Cells Spheroids into Lockyballs. *PLoS One* **11**, e0166073 (2016).
68. Correia, C. R., Gil, S., Reis, R. L. & Mano, J. F. A Closed Chondromimetic Environment within Magnetic-Responsive Liquified Capsules Encapsulating Stem Cells and Collagen II/TGF-β3 Microparticles. *Adv. Healthc. Mater.* **5**, 1346–1355 (2016).
69. Duan, B., Shou, K., Su, X., Niu, Y., Zheng, G., Huang, Y., Yu, A., Zhang, Y.,

Xia, H. & Zhang, L. Hierarchical Microspheres Constructed from Chitin Nanofibers Penetrated Hydroxyapatite Crystals for Bone Regeneration. *Biomacromolecules* **18**, 2080–2089 (2017).

70. Correia, C. R., Santos, T. C., Pirraco, R. P., Cerqueira, M. T., Marques, A. P., Reis, R. L. & Mano, J. F. In vivo osteogenic differentiation of stem cells inside compartmentalized capsules loaded with co-cultured endothelial cells. *Acta Biomater.* **53**, 483–494 (2017).
71. Correia, C. R., Pirraco, R. P., Cerqueira, M. T., Marques, A. P., Reis, R. L. & Mano, J. F. Semipermeable Capsules Wrapping a Multifunctional and Self-regulated Co-culture Microenvironment for Osteogenic Differentiation. *Sci. Rep.* **6**, 21883 (2016).
72. Mealy, J. E., Chung, J. J., Jeong, H.-H., Issadore, D., Lee, D., Atluri, P. & Burdick, J. A. Injectable Granular Hydrogels with Multifunctional Properties for Biomedical Applications. *Adv. Mater.* **30**, 1705912 (2018).
73. Chen, M. H., Chung, J. J., Mealy, J. E., Zaman, S., Li, E. C., Arisi, M. F., Atluri, P. & Burdick, J. A. Injectable Supramolecular Hydrogel/Microgel Composites for Therapeutic Delivery. *Macromol. Biosci.* **19**, 1800248 (2018).
74. Ferreira, L. P., Gaspar, V. M. & Mano, J. F. Design of spherically structured 3D in vitro tumor models -Advances and prospects. *Acta Biomater.* **75**, 11–34 (2018).
75. Yamada, M., Hori, A., Sugaya, S., Yajima, Y., Utoh, R., Yamato, M. & Seki, M. Cell-sized condensed collagen microparticles for preparing microengineered composite spheroids of primary hepatocytes. *Lab Chip* **15**, 3941–3951 (2015).
76. Jakob, P. H., Kehrer, J., Flood, P., Wiegel, C., Haselmann, U., Meissner, M., Stelzer, E. H. K. & Reynaud, E. G. A 3-D cell culture system to study epithelia functions using microcarriers. *Cytotechnology* **68**, 1813–25 (2016).
77. Skardal, A., Sarker, S. F., Crabbé, A., Nickerson, C. A. & Prestwich, G. D. The generation of 3-D tissue models based on hyaluronan hydrogel-coated microcarriers within a rotating wall vessel bioreactor. *Biomaterials* **31**, 8426–8435 (2010).
78. Bratt-Leal, A. M., Nguyen, A. H., Hammersmith, K. A., Singh, A. & McDevitt, T. C. A microparticle approach to morphogen delivery within pluripotent stem cell aggregates. *Biomaterials* **34**, 7227–7235 (2013).
79. Zhang, Y., Mao, H., Gao, C., Li, S., Shuai, Q., Xu, J., Xu, K., Cao, L., Lang, R.,

Gu, Z., Akaike, T. & Yang, J. Enhanced Biological Functions of Human Mesenchymal Stem-Cell Aggregates Incorporating E-Cadherin-Modified PLGA Microparticles. *Adv. Healthc. Mater.* **5**, 1949–1959 (2016).

80. Ahmad, T., Lee, J., Shin, Y. M., Shin, H. J., Madhurakat Perikamana, S. K., Park, S. H., Kim, S. W. & Shin, H. Hybrid-spheroids incorporating ECM like engineered fragmented fibers potentiate stem cell function by improved cell/cell and cell/ECM interactions. *Acta Biomater.* **64**, 161–175 (2017).
81. Bratt-Leal, A. M., Carpenedo, R. L., Ungrin, M. D., Zandstra, P. W. & McDevitt, T. C. Incorporation of biomaterials in multicellular aggregates modulates pluripotent stem cell differentiation. *Biomaterials* **32**, 48–56 (2011).
82. Baraniak, P. R., Cooke, M. T., Saeed, R., Kinney, M. A., Fridley, K. M. & McDevitt, T. C. Stiffening of human mesenchymal stem cell spheroid microenvironments induced by incorporation of gelatin microparticles. *J. Mech. Behav. Biomed. Mater.* **11**, 63–71 (2012).
83. Abbasi, F., Ghanian, M. H., Baharvand, H., Vahidi, B. & Eslaminejad, M. B. Engineering mesenchymal stem cell spheroids by incorporation of mechanoregulator microparticles. *J. Mech. Behav. Biomed. Mater.* **84**, 74–87 (2018).
84. Yue, S., Sun, X., Wang, N., Wang, Y., Wang, Y., Xu, Z., Chen, M. & Wang, J. SERS–Fluorescence Dual-Mode pH-Sensing Method Based on Janus Microparticles. *ACS Appl. Mater. Interfaces* **9**, 39699–39707 (2017).
85. Shin, D. S., Tokuda, E. Y., Leight, J. L., Miksch, C. E., Brown, T. E. & Anseth, K. S. Synthesis of Microgel Sensors for Spatial and Temporal Monitoring of Protease Activity. *ACS Biomater. Sci. Eng.* **4**, 378–387 (2018).
86. Barrila, J., Yang, J., Crabbé, A., Sarker, S. F., Liu, Y., Ott, C. M., Nelman-Gonzalez, M. A., Clemett, S. J., Nydam, S. D., Forsyth, R. J., Davis, R. R., Crucian, B. E., Quiriarte, H., Roland, K. L., Brenneman, K., Sams, C., Loscher, C. & Nickerson, C. A. Three-dimensional organotypic co-culture model of intestinal epithelial cells and macrophages to study Salmonella enterica colonization patterns. *npj Microgravity* **3**, 10 (2017).
87. Kolesky, D. B., Truby, R. L., Gladman, A. S., Busbee, T. A., Homan, K. A. & Lewis, J. A. 3D Bioprinting of Vascularized, Heterogeneous Cell-Laden Tissue Constructs. *Adv. Mater.* **26**, 3124–3130 (2014).
88. Neufurth, M., Wang, X., Wang, S., Steffen, R., Ackermann, M., Haep, N. D.,

Schröder, H. C. & Müller, W. E. G. 3D printing of hybrid biomaterials for bone tissue engineering: Calcium-polyphosphate microparticles encapsulated by polycaprolactone. *Acta Biomater.* **64**, 377–388 (2017).

89. Zhong, M., Sun, J., Wei, D., Zhu, Y., Guo, L., Wei, Q., Fan, H. & Zhang, X. Establishing a cell-affinitive interface and spreading space in a 3D hydrogel by introduction of microcarriers and an enzyme. *J. Mater. Chem. B* **2**, 6601–6610 (2014).
90. Tan, Y. J., Tan, X., Yeong, W. Y. & Tor, S. B. Hybrid microscaffold-based 3D bioprinting of multi-cellular constructs with high compressive strength: A new biofabrication strategy. *Sci. Rep.* **6**, 39140 (2016).
91. Roh, S., Parekh, D. P., Bharti, B., Stoyanov, S. D. & Velev, O. D. 3D Printing by Multiphase Silicone/Water Capillary Inks. *Adv. Mater.* **29**, 1701554 (2017).
92. Highley, C. B., Song, K. H., Daly, A. C. & Burdick, J. A. Jammed Microgel Inks for 3D Printing Applications. *Adv. Sci.* **6**, 1801076 (2018).
93. Wang, C., Gong, Y., Zhong, Y., Yao, Y., Su, K. & Wang, D.-A. The control of anchorage-dependent cell behavior within a hydrogel/microcarrier system in an osteogenic model. *Biomaterials* **30**, 2259–2269 (2009).
94. Neufurth, M., Wang, X., Wang, S., Steffen, R., Ackermann, M., Haep, N. D., Schröder, H. C. & Müller, W. E. G. 3D printing of hybrid biomaterials for bone tissue engineering: Calcium-polyphosphate microparticles encapsulated by polycaprolactone. *Acta Biomater.* **64**, 377–388 (2017).
95. Mekhileri, N. V, Lim, K. S., Brown, G. C. J., Mutreja, I., Schon, B. S., Hooper, G. J. & Woodfield, T. B. F. Automated 3D bioassembly of micro-tissues for biofabrication of hybrid tissue engineered constructs. *Biofabrication* **10**, 024103 (2018).
96. Hospodiuk, M., Dey, M., Sosnoski, D. & Ozbolat, I. T. The bioink: A comprehensive review on bioprintable materials. *Biotechnol. Adv.* **35**, 217–239 (2017).
97. Schmidt, J. J., Jeong, J. & Kong, H. The Interplay Between Cell Adhesion Cues and Curvature of Cell Adherent Alginate Microgels in Multipotent Stem Cell Culture. *Tissue Eng. Part A* **17**, 2687–2694 (2011).
98. Griffin, D. R., Weaver, W. M., Scumpia, P. O., Di Carlo, D. & Segura, T. Accelerated wound healing by injectable microporous gel scaffolds assembled from annealed building blocks. *Nat. Mater.* **14**, 737–744 (2015).

99. Li, F., Truong, V. X., Fisch, P., Levinson, C., Glattauer, V., Zenobi-Wong, M., Thissen, H., Forsythe, J. S. & Frith, J. E. Cartilage tissue formation through assembly of microgels containing mesenchymal stem cells. *Acta Biomater.* **77**, 48–62 (2018).
100. Kamperman, T., Henke, S., van den Berg, A., Shin, S. R., Tamayol, A., Khademhosseini, A., Karperien, M. & Leijten, J. Single Cell Microgel Based Modular Bioinks for Uncoupled Cellular Micro- and Macroenvironments. *Adv. Healthc. Mater.* **6**, 1600913 (2017).
101. Graham, A. D., Olof, S. N., Burke, M. J., Armstrong, J. P. K., Mikhailova, E. A., Nicholson, J. G., Box, S. J., Szele, F. G., Perriman, A. W. & Bayley, H. High-Resolution Patterned Cellular Constructs by Droplet-Based 3D Printing. *Sci. Rep.* **7**, 7004 (2017).
102. Zhong, M., Wei, D., Yang, Y., Sun, J., Chen, X., Guo, L., Wei, Q., Wan, Y., Fan, H. & Zhang, X. Vascularization in Engineered Tissue Construct by Assembly of Cellular Patterned Micromodules and Degradable Microspheres. *ACS Appl. Mater. Interfaces* **9**, 3524–3534 (2017).
103. Matsunaga, Y. T., Morimoto, Y. & Takeuchi, S. Molding Cell Beads for Rapid Construction of Macroscopic 3D Tissue Architecture. *Adv. Mater.* **23**, H90–H94 (2011).
104. Sheikhi, A., de Rutte, J., Haghniaz, R., Akouissi, O., Sohrabi, A., Di Carlo, D. & Khademhosseini, A. Microfluidic-enabled bottom-up hydrogels from annealable naturally-derived protein microbeads. *Biomaterials* **192**, 560–568 (2019).
105. Lee, B. W., Liu, B., Pluchinsky, A., Kim, N., Eng, G. & Vunjak-Novakovic, G. Modular Assembly Approach to Engineer Geometrically Precise Cardiovascular Tissue. *Adv. Healthc. Mater.* **5**, 900–906 (2016).
106. Sun, T., Shi, Q., Huang, Q., Wang, H., Xiong, X., Hu, C. & Fukuda, T. Magnetic alginate microfibers as scaffolding elements for the fabrication of microvascular-like structures. *Acta Biomater.* **66**, 272–281 (2018).
107. Ma, S., Mukherjee, N., Mikhailova, E. & Bayley, H. Gel Microrods for 3D Tissue Printing. *Adv. Biosyst.* **1**, 1700075 (2017).
108. Yang, W., Yu, H., Li, G., Wang, Y. & Liu, L. High-Throughput Fabrication and Modular Assembly of 3D Heterogeneous Microscale Tissues. *Small* **13**, 1602769 (2017).

Chapter II*

Materials and Methods

*This chapter consists of a full detailed description and explanation of both materials and experimental procedures adopted to produce quasi-2D shape tailored microparticles *via* pre-patterned platforms of extreme wettabilities. The methodologies selected to assess morphological, topographical and morphometric features of the sheet-like particles are also herein detailed, as wells as, the ones used to properly evaluate their biological performance within cell aggregates.

II.1. Materials

Dichloromethane (DCM), Cysteamine hydrochloride (≥97.0% purity), Poly acrylic acid (PAA, M_n ~450,000), Poly-ε-caprolactone (PCL, M_n 80,000), Polystyrene (PS, M_n ~192,000), Coumarin-6 (Coum-6, 98% purity), Tetrahydrofuran (THF, 250 ppm BHT, ≥99.9%), sodium hydroxide (NaOH) and Dulbecco's phosphate-buffered saline (DPBS), Trypsin-EDTA and formaldehyde solutions were all purchase from Laborspirit (Lisbon, Portugal). Sulphuric acid (H_2SO_4, 95-97% purity), Triethylamine (TEA, 99% purity), 4-(dimethylamine)pyridine (DMAP, 99% purity) and Ethyl acetate (EA, 99-100%) were purchased from JMGS Lda. (Odivelas, Portugal). Chloro(dimethyl)vinylsilane (>97% purity) and Nile Red were purchased from TCI Chemicals (Tokyo, Japan). 1H,1H,2H,2H-Perfluorodecanethiol (PFDT, 97% purity) was purchased from CYMIT Química S.L. (Barcelona, Spain). Quartz chromium photomask and quartz slide were both developed and manufactured by JD Photo-Data (Hitchin, UK). UV/Ozone Procleaner™ (220V) was acquired from BioForce Nanosciences (Utah, USA). Human adipose stem cells (hASCs, passages – between P6 and P8) hASCs were isolated from adipose tissue. The retrieval and transportation of the samples to the laboratorial facilities was performed under a protocol previously established with the Hospital da Luz (Aveiro, Portugal) and approved by the local Ethical Committee. Minimum Essential Medium α-modification (α-MEM, -nucleosides, +L-glutamine), AlamarBlue™, Live/Dead Kit and 4',6-diamidino-2-phenylindole, dihydrochloride (DAPI) were purchased from Alfagene (Lisbon, Portugal). Flash Phalloidin™ Red 594 was purchased from Biolegend (California, USA). Human VEGF ELISA kit (ab100662) was purchase from Abcam.

II.2. Methods

II.2.1. Fabrication of wettability contrast-based microarrays for low-surface-tension liquids

Bare glass slides were first activated to promote surface hydroxylation by immersing them overnight in an oxidizing acid – H_2SO_4 – at RT followed by an extensive wash with H_2O to remove any acid remnants. The surface modification and the dewetting-

wetting pattern was attained following a previously described method with some minor modifications[1]. First, the pre-hydroxylated glass slides were subjected to a silanization reaction. This reaction was conducted in a DCM solution containing TEA (1.6% (v/v)), DMAP (1 mg mL^{-1}) and chloro(dimethyl)vinylsilane (0.4% (v/v)) for 5 min under continuous stirring and at RT. The organofunctional silane grafting endowed the glass surface with a thiol-reactive monolayer of vinyl groups. After washing the vinyl-modified surface in ethanol and dried under a stream of nitrogen, a spatially-controlled, non-wettable pattern of fluorinated areas was imprinted in the slide via a thiol-ene click reaction in a 30% (v/v) PFDT in a EA solution for 1 min under UV irradiation through a quartz chromium photomask that enables a site-selective exposure of the surface to the light source, controlling the reaction location. Once the reaction was completed, the resulting glass was cleaned with acetone to wash-off any fluorinated residues and dried with a stream of nitrogen. Lastly, the remaining unmodified vinyl groups were further functionalized to create wettable micropatterns with cysteamine hydrochloride, via a thiol-ene reaction. This way, and adopting a photolithographic strategy, an array of pre-defined and patterned amine spots that are wettable alternated with a fluorinated areas capable of dewetting several organic solvents was created. The overall procedure is depicted in Figure II.1.

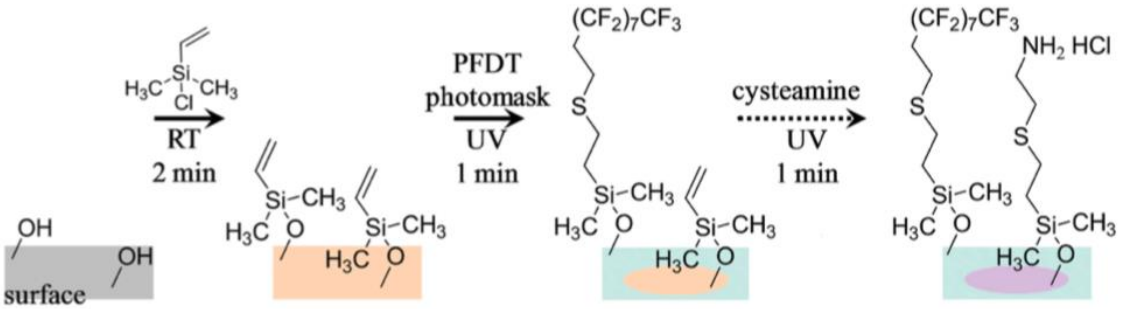

Figure II.1. Schematic representation of the overall surface functionalization for the creation of wettable-dewettable micropatterns. First, the silanization reaction is conducted to render vinyl groups at the surface, that will, in a second step, react through an UV-induced thiol-ene click chemistry reaction with PFDT, under site-selective exposer through a photomask. The unmodified vinyl groups are then, further functionalized with cysteamine hydrochloride, via the same reaction chemistry as before. The resulted surface exhibits regio-selective domains of amine groups and fluorinated areas. Adapted from [1].

II.2.2. Preparation of quasi-2D shape-tailored microparticles

As aforementioned, these platforms comprises two distinct regions based on wettability by organic liquids. Therefore, as they exhibit two extreme and contrasting wettability areas, they are able to both repel and hold those liquids and generate an array of surface-tension-confined microdroplets. While in the domains showing a good wettability, they can hold the liquid and pin it to the surface, around the contact baseline of the pattern, perfectly recreating the exact design predefined by photolithography; in the areas showing a good dewettability, thus a bad wettability, the liquid simply just "roll-off" the surface. This process is known as discontinuous dewetting[1]. Moreover, to efficiently dewet the liquid from the surface, this is preferably to be performed with a certain degree of inclination which, driven by gravitational forces, helps to remove the excess liquid[2]. Hence, a dip-coating method is the most appealing to this strategy. Exploiting such particular features, these surfaces were envisioned to be used as platforms to create flat, sheet-like particles with different size and shape designs, where the patterned array is used as guiding template for deposition of organic soluble polymers[3]. This approach comprises two different processes based on (i) the dip-coating in a polymer solution and (ii) polymer deposition through solvent evaporation. Furthermore, to easily remove the polymer layer deposited in the surface, a sacrificial template strategy was employed.

II.2.2.1. Sacrificial layer

The strategy to engender such quasi-2D microparticles encompasses the generation of a first layer, designed to be later removed, as a sacrificial template. In this sense, the patterned glass was dip-coated in a 2% (w/v) PAA solution prepared in ethanol and further diluted in distilled water at a ratio of 7:3. Through solvent evaporation, the polymer deposited within the patterned domains.

II.2.2.2. Microparticle production

To fabricate the microparticles, the dip-coating procedure and solvent evaporation steps are repeated. In this work, was used PCL (2%, 3.5% and 5% (w/v) in DCM) as the backbone of the particles, as a proof-of-concept of the methodology. Although, to demonstrate the versatility of the organic soluble polymers that can be employed, we also

fabricated PS microparticles (5% (w/v) in THF).

II.2.2.3. Freestanding microparticles

The term freestanding in here is employed to refer to structures that do not require full contact with a solid substrate to maintain their shape integrity or physical properties[4]. So, in this work, to generate freestanding microparticles, the whole assembly was immersed into a 1 M aqueous solution of NaOH. This causes the sacrificial layer to dissolve, and the microparticles to be release from the glass surface into the solution where they stay in suspension while retaining their shape and whole integrity. Due to the pH-responsiveness of the PAA, upon increasing of pH, ionization of the polymer occurs and the polymer expands from a globular conformation into a fully solvated open coil conformation[5]. This increased the exposer of the PAA to the alkaline solution which etched and disintegrated the layer, leading to the lift-off of the particles from the surface[6]. After three hours in an alkaline solution is possible to see the entire set/array of particles detached from the substrate. Additional mechanical stimulation, such as agitation or creating a continuous flow with pipetting can quicken the process. The particles were left overnight in the solution to increase the particles' surface energy and enhance hydrophilicity and to achieve better cell adhesion since PCL lacks proper functional groups for cells to interact with. The synergistic effect of the enhanced exposed surface with the higher hydrophilicity improve greatly the adhesiveness of the material[7].

II.2.3. Microparticle characterization

II.2.3.1. 3D Optical Profiler

Microparticles morphology, thickness, and morphometric features such as size and shape fidelity (roundness for circular particles and aspect ratio for square particles) according to the photomask used were assessed by optical profilometry following the international standard procedure dictated by ISO 25178 Surface Texture. The roundness of both on-chip and freestanding particles was calculated using ImageJ Software (v1.52n), through the following equation, where a perfect circle will exhibit a roundness of 1:

$$Roundness = 4\frac{Area}{\pi(Major\ Axis)^2} \quad (1)$$

S Neox and Sensofar Metrology software was used to acquire the images of the deposition of both polymers, using the following set-ups: Phase-Shift Interferometer (PSI), 10x DI. With this methodology is possible to acquire 3D profile images through a non-contact fashion, which allows a precise scanning without damaging the sample, and also makes possible to measure large fields at once, without losing any height resolution. PSI is indicated to measure surface heights of very smooth and continuous surfaces, such as the ones of plastic films and micromirrors. SensoSCAN 6.0 software was used to process and analyze all the data acquired with the equipment. For Profilometry analysis, the on-chip and freestanding microparticles were both evaluated in RT and under atmospheric air. For the on-chip particles, the morphology assessed concerns the assembly of the PCL microparticles with the PAA sacrificial layer beneath (PAA + PCL deposition). Regarding the freestanding microparticles, the PCL particles were detached as described above, washed with distilled water to remove any NaOH remnants until reach a proximal to neutral pH, and then washed with ethanol and dispersed in a microscope glass slide until the solvent completely evaporates from the surface. For every parameter study a minimum of 75 particles were analyzed. For every condition stated a polydispersity index was calculated to assessed the monodispersity in thickness of the particles produce, using the following equation[8], where s.d. is the standard deviation and mean is the arithmetic mean of the thickness measured:

$$PDI = \left(\frac{s.d.}{mean}\right)^2 \quad (2)$$

II.2.4. In vitro cell culture

All cells used in this work were cultured in aseptic conditions and the entire procedure related to the biological assays were performed in a laminar flow chamber, when needed, to prevent sample contamination. Human adipose-derived stem cells (hASCs) were cultured in α-MEM supplemented with sodium bicarbonate, 10% (v/v) heat-inactivated Fetal Bovine Serum (FBS) and 1% (v/v) of an antibiotic and antimycotic (penicillin-

streptomycin) at pH 7.2. Cells were grown and expanded in 175cm^2 tissue culture flask and incubated at 37ºC in a humidified 5% CO_2 atmosphere. Cells were sub-cultured before reaching full confluency and passages between P6-P8 were used. Cellular suspensions were prepared via enzymatic detachment of cells from tissue culture plastic with a Trypsin/EDTA solution, incubated for 5 min at 37ºC, after which was added fresh medium to the suspension in order to inactivate the trypsin and centrifuged at 300 x g and 25ºC for 5 min. The supernatant was discarded and cells were resuspended with fresh media. To generate hASCs aggregates, cells were cultured in ultra-low attachment (ULA, Corning® Costar®), clear round bottom 96-well plates at a density of 10.000 cells/well. For "hybrid" aggregates, cells were cultured with microparticles. Prior to each assay, PCL microparticles were detached as previously described and left overnight in alkaline solution to enhance hydrophilicity and cell attachment before an extensive wash in DPBS and distributed to each well at a density of 30-50 particles/well and sterilized under UV light for 30 min. Self-aggregation and spheroid formation was visible after 24 h of culture and monitored over time within 3 days.

II.2.5. Biological performance of microparticles

II.2.5.1. Cell viability

II.2.5.1.1. Live/Dead assay

This assay is an easy-to-do and fast procedure that allows the simultaneous staining of both live and dead cells in an one-step approach, visible under fluorescence microscopy. Live/Dead assay is based on two highly fluorescent dyes that differentially label live and dead cells: The live cell dye, acetomethoxy derivative of calcein (Calcein AM), is a non-fluorescent and hydrophobic dye that can easily permeate intact membranes of viable cells. Once inside the cytosol the dye will invariably encounter esterases capable of cleave the ester bonds present in the Calcein AM structure, converting it into Calcein, which displays a green fluorescence. The dead cell dye, propidium iodide (PI), is a red-fluorescent hydrophilic dye that is not permeant to live cells. If the membrane is compromised, the dye can enter the cell and bind with high-affinity to nucleic acids, by intercalating between the bases with little to no preference sequence, staining them as bright red.

In this work, Live/Dead assay was performed at pre-determined time points, 24 and 72 hours after cell culturing. Cell-only spheroids and Cell-particle spheroids were incubated in a mixed solution of 2 μL of Calcein AM (1 mg mL^{-1}) and 1 μL of PI (1 mg mL^{-1}) in 1 mL of PBS at 37ºC over 30 minutes. Prior to this, spheroids were washed three times with PBS to completely remove the cell culture medium and prevent possible esterase activity outside the cells. Images were acquired through fluorescence microscopy (Zeiss Axio Imager M2, Carl Zeiss Microscopy GmbH).

II.2.5.1.2. Cellular metabolic activity quantification

The viability and metabolic activity of cells within spheroids (cells-only and cells-particles aggregation) were quantitatively measured by AlamarBlue™ cell viability assay. According to ThermoFisher Scientific, in healthy cell conditions, the active compound, resazurin, which is blue in color and non-fluorescent, can be internalized by cells. Afterwards, inside the healthy living cells, due to their reduced environment, resazurin is reduced into resofurin, which is red in color and highly fluorescent[9]. The viabibility and metabolic activity were assessed after 24 and 72 hours of culture. In this regard, a 10% (v/v) solution of AlamarBlue™ reagent was prepared in previously warmed and supplemented α-MEM, transferred into the round-bottom well-plates, and incubated at 37ºC overnight. Following the incubation period, the media was then transferred to a black clear bottom 96-well plate for analysis. AlamarBlue™ fluorescence was detected at an excitation wavelength of 540/35 nm and at an emission wavelength of 600/40 nm by using a microplate reader (Synergy™ HT, Bio-Tek Instruments, Inc.). The particle containing spheroids were normalized to the control group (cell-only spheroids) set at 100% viability.

II.2.5.2. Cell-microparticle aggregation morphology

II.2.5.2.1. Morphometric features

The basic morphometric features such as diameter, circularity and roundness[10] exhibited by micrographs of the spheroids acquired at specific timepoints (n=4), were processed and calculated in ImageJ Software (v1.52n). Circularity was calculated by equation (3), and roundness by equation (1). A perfect circle will exhibit a circularity of 1.

$$Circularity = 4\pi\left(\frac{Area}{Perimeter^2}\right) \quad (3)$$

II.2.5.2.2. Nuclei and actin filament staining

To characterize cell morphology, the nuclei (blue) was stained with DAPI (1 mg mL^{-1}, 1 : 1000 ratio in PBS for 30 min, RT) and actin filament (red) stained with phalloidin (Flash Phalloidin™ Red 594, 300U, BioLegend, 1 : 40 ratio in PBS for 60 min, RT) posteriorly to cell fixation with 4% (v/v) formaldehyde solution in PBS for 20 min at RT and permeabilization with 0.1% (v/v) Triton X-100 in PBS for 10 minutes. Afterwards, the samples were washed three times in PBS and observed by fluorescence microscopy (Zeiss Axio Imager M2, Carl Zeiss Microscopy GmbH) and confocal laser scanning microscopy (Zeiss LSM 510 Meta, Zeiss LSM 880 Airyscan, Carl Zeiss Microscopy GmbH), where samples were excited with different laser units: Diode 405-30 at a wavelength of 405 nm, Argon/2 at 488 nm and DPSS 561-10 at 561 nm. Imaging processing was performed using ImageJ Software (v1.52n).

II.2.5.2.3. Scanning Electron Microscopy (SEM)

To further explore the morphology of both particles and cells within the whole aggregate an analysis on a high-resolution field microscope (SU-70, Hitachi) operated in the secondary electrons mode at accelerating voltages 15.0 kV and working distance of 14.9 mm. Prior to the analysis, all samples were fixed as aforementioned and washed 3 times with PBS and then dehydrated in increasing ethanol series, starting at 10% (v/v) up to 100% (v/v) with increments of 10%. Each incubation in ethanol series lasted for 10 min and it was performed at ambient temperature. After, samples were air-dried and mounted on aluminum stubs by double-sided carbon conductive adhesive tape, cross-sectioned and further coated with a layer of carbon using a sputter coater (Emitech K950x).

II.2.5.3. Enzyme-linked Immunosorbent Assay (ELISA) - Quantification of VEGF

ELISA is a simple, easy to design and perform immunoassay, convenient for detecting and quantifying the exact concentration of particular substrates, such as peptides and/or

proteins, from a heterogeneous population. ELISA assay combines the specificity of antibodies with the sensitivity of enzymes, where the detection of a certain substrate is quantified through a development of a certain color, if present. Amid the different types of ELISA assays, the "sandwich" type is described as the most powerful and sensitive format, where the detection principle is based on the capture of the analyte between two primary antibodies – the pre-immobilized capture antibody and the enzyme-linked detection antibody – where the latter can catalyze a given substrate and develop a colored product, proportional to the amount of the target protein in the sample.

In this work, the release of growth factors into cell medium was evaluated after 1 and 3 days of culture, both in exclusively cell spheroids and in particle embedded cell spheroids (n=4), by sandwich ELISA detection method for quantification of VEGF (Human VEGF ELISA kit, ab100662), following the manufacturer's instructions. Prior to this, cell medium supernatant was quickly centrifuged at 1500 rpm for 10 min at 4ºC to remove any precipitate or cellular debris. After all the incubation and procedure steps, the VEGF levels were quantified UV-VIS analysis at λ = 450 nm using a microplate reader (Synergy^{TM} HT, Bio-Tek Instruments, Inc.). The results were plot and fitted on a four parameter logistic curve.

II.2.6. Statistical analysis

All data statistical analysis was conducted using GraphPad Prism v6.0 software. Results are expressed as mean ± standard deviation (s.d.). The statistical analysis was performed using two-way ANOVA test, followed by a Tukey's multiple comparisons test for pairwise comparison. Statistical significances were established for *p-values* < 0.05. The results are non-significantly unless otherwise marked with asterisk character (*).

II.3. References

1. Feng, W., Li, L., Du, X., Welle, A. & Levkin, P. A. Single-Step Fabrication of High-Density Microdroplet Arrays of Low-Surface-Tension Liquids. *Adv. Mater.* **28**, 3202–3208 (2016).

2. Chen, X., Wu, H. & Wu, J. Surface-tension-confined droplet microfluidics. *Chinese Physics B* vol. 27 (2018).

3. Kobaku, S. P. R., Kwon, G., Kota, A. K., Karunakaran, R. G., Wong, P., Lee, D. H. & Tuteja, A. Wettability Engendered Templated Self-assembly (WETS) for Fabricating Multiphasic Particles. *ACS Appl. Mater. Interfaces* **7**, 4075–4080 (2015).

4. Jiang, C. & Tsukruk, V. V. Freestanding Nanostructures via Layer-by-Layer Assembly. *Adv. Mater.* **18**, 829–840 (2006).

5. Swift, T., Swanson, L., Geoghegan, M. & Rimmer, S. The pH-responsive behaviour of poly(acrylic acid) in aqueous solution is dependent on molar mass. *Soft Matter* **12**, 2542–2549 (2016).

6. Gao, Y., Xu, W. & Serpe, M. J. Free-standing poly (N-isopropylacrylamide) microgel-based etalons. *J. Mater. Chem. C* **2**, 5878–5884 (2014).

7. Chen, F., Lee, C. N. & Teoh, S. H. Nanofibrous modification on ultra-thin poly(e-caprolactone) membrane via electrospinning. *Mater. Sci. Eng. C* **27**, 325–332 (2007).

8. Danaei, M., Dehghankhold, M., Ataei, S., Hasanzadeh Davarani, F., Javanmard, R., Dokhani, A., Khorasani, S. & Mozafari, M. R. Impact of particle size and polydispersity index on the clinical applications of lipidic nanocarrier systems. *Pharmaceutics* vol. 10 (2018).

9. Rampersad, S. N. Multiple applications of alamar blue as an indicator of metabolic function and cellular health in cell viability bioassays. *Sensors (Switzerland)* **12**, 12347–12360 (2012).

10. Yu, H., Lim, K. P., Xiong, S., Tan, L. P. & Shim, W. Functional morphometric

analysis in cellular behaviors: Shape and size matter. *Advanced Healthcare Materials* vol. 2 1188–1197 (2013).

Chapter III*

Results and Discussion

*This chapter is based on the article entitled
“Fabrication of quasi-2D shape-tailored microparticles using wettability contrast-based platforms”
(manuscript under preparation)

Fabrication of quasi-2D shape-tailored microparticles using wettability contrast-based platforms

Mafalda D. Neto[1], Aukha Stoppa[1,2], Miguel A. Neto[1], Filipe J. Oliveira[1], Maria C. Gomes[1], Aldo R. Bocaccini[2], Pavel A. Levkin[3], Mariana B. Oliveira[1,*], João F. Mano[1,*]

[*]Correspondence: M.B. Oliveira: mboliveira@ua.pt; J.F. Mano: jmano@ua.pt

[1]*Department of Chemistry, CICECO – Aveiro Institute of Materials. University of Aveiro. Campus Universitário de Santiago. 3810-193 Aveiro, Portugal*

[2]*Institute of Biomaterials, Department of Materials Science and Engineering, University of Erlangen-Nuremberg, 91058 Erlangen, Germany*

[3]*Karlsruhe Institute of Technology, Institute of Organic Chemistry, Fritz-Haber Weg 6, 76131 Karlsruhe, Germany*

III.1. Abstract

The discovery of two-dimensional (2D) materials led to the breakthrough of a multitude of different low dimensional structures with very unique properties, namely (i) high surface area-to-volume ratio, (ii) sub-micrometer thickness, (iii) heterofunctionality and (iv) non-covalent adhesiveness, which surpass their bulk counterparts. Although their development regarding tunable lateral-dimensions and geometries remains challenging, pre-patterned platforms had gain significant attention in addressing such drawback. Herein, resorting to wettability contrast patterned surfaces, different nanometer-thick particles of various sizes and geometries (e.g. squares, circles, triangles, hexagons) with high precision and definition were developed. These ultrathin quasi-2D polymeric microparticles in contact with cells allow the generation of gravity-enforced human adipose-derived stems cells spheroids without impairing their natural morphology. Cells remain viable following 3 days in culture, metabolically active and show an increase in release of angiogenic factors, namely VEGF.

Keywords: ultrathin microparticles, quasi-2D polymeric nanostructures, patterned surfaces, wettable-dewettable contrasts

III.2. Steering 2D materials as novel future modulators

Since the discovery of graphene, in 2004, significant interest in ultrathin materials have broken out which has led to intensive research and the discovery of a whole family of 2D materials, including transition metals oxides and dichalcogenides, boron nitride and several others, with promising features that can find purpose in countless fields [1,2]. This has also brought into focus the design of other low dimensional structures composed of distinct materials, e.g. polymers. Owing to their reduced thickness, their physical and chemical properties can be significantly altered resulting in unique features that outperforms bulk polymeric materials [3]. Among these exceptional features, the most prevalent is their (i) high aspect ratio and high surface area-to-volume ratio that these types of materials exhibit. The enhanced surface becomes more important and even more dominant compared to their bulk counterparts which adapts them as potential candidates for numerous applications, namely, as sensors or even as catalytic platforms for the scale-up of reactions, owing to their maximized surface area with abundant exposed active site moieties[4]. Other exciting applications include scavenging platforms, such as energy harvesting systems[5] or even as adsorbents[6] able to effectively capture and isolate, via chemical affinity, contaminants or other species of interest in order to purify any given system. Furthermore, the extensive interface displayed by these flat materials can also act as surfactants that help stabilize the so-called Pickering emulsions, in which a physical barrier between the two immiscible phases prevents droplet coalescence preserving their 'balanced' dispersion within the continuous phase[7]. This class of materials, as previously stated, also presents an (ii) extremely reduced thickness, ranging from tens to several hundred of nanometers, naming them as ultrathin films[3,8]. As a result, they fall into a novel category of soft nanostructured materials, which behave in a thickness-dependent manner and show a remarkably high flexibility. Such compliant nature can be appealing to many different applications ranging from wearable soft electronics[9] to injectable systems in Regenerative Medicine strategies, as minimally invasive implantation procedures[8,10]. Moreover, envisioning the creation of more intricate and sophisticated structures, these highly pliable 'sheets' can be programmed and manipulated, through folding or bending, into origami-inspired three-dimensional (3D) assemblies, adding extra value and function [11–13]. Another particular feature is their (iii) heterofunctionality, as they present two opposing interfaces plausible to be tailored in order to present asymmetric properties on each side, resulting in different functions, all in one[6,14]. The

design of these Janus-type materials can be through different structures (e.g. roughness), composition (e.g. different materials) or even polarity (e.g. hydrophobicity). It has also been reported their potential as a tissue sealant to replace surgical sutures due to their (iv) non-covalent adhesiveness where no chemically-bond agent is required, and the adherence is purely physical[15]. This property is conveniently interesting when the tissue is badly or severely damaged, as in cases of burn wounds, where sutures are impractical and challenging to do, and also act as a physical barrier against infections[16].

Among several techniques to assemble nanometer-level materials there are a few noteworthy to mention, being the common practice: Layer-by-Layer (LbL) technology[17] and the Langmuir-Blodgett method[18]. Both systems present excellent thickness control in the nanoscale, which allows to fabricate complex architectures at the molecular level. However, they are time-consuming and require multiple steps, taking up many hours up to several days to achieve. Another methods, such as spin- and dip-coating may provide a simpler and faster way to assemble freestanding ultrathin structures based on a combination of, either a (i) sacrificial layer or a (ii) cast/supporting layer technique with a followed single step polymer deposition[19,20]. Despite the advantages offered by the aforementioned techniques, they still lack control over lateral size at a micrometer-scale and geometry. Therefore, approaches based on pre-patterned platforms offer not only potential to control the lateral dimensions of the material but also control of the overall shape[21,22].

Hence, in this work we developed monodispersed ultrathin quasi-2D polymeric particles with only several hundreds nanometers in thickness and a specific range of micrometers in lateral size (50-500 μm) with a sorted of different geometries resorting to a high-density microdroplet array of low-surface-tension liquids[23]. Adopting such pre-patterned surface, we demonstrate an easy and straightforward method to produce highly tailorable microparticles, compliant with large scalability. These sheet-like particles with enhanced surface-to-volume-ratio proved to support cell adhesion and expansion within spheroids, thus acting as cell carriers.

III.3. Wettability contrast platforms to develop quasi-2D particles

Arrays of a micropatterned surface compatible with several organic liquids were prepared as previously described[23] to enable the fabrication of polymeric quasi-2D particles. Such arrays encompass wettable spots of geometrically defined patterns within

a non-wettable region. While the latter region repels the liquid or solution, the first, driven by surface tension, can hold it and pin it to the surface, perfectly matching the frame of the patterns, in a process known as discontinuous dewetting. Exploiting this attribute, the wettable domains are used as templates to guide the polymer solutions into forming the corresponding shape. In this sense, we developed a methodology based on a sequential dip-coating process into two different solvent-soluble polymer solutions, where the first acts as a sacrificial layer to be later removed, consequently leading to the release of the second layer as freestanding structure. The overall experimental procedure is depicted in Figure 1a. First, the pristine pre-patterned surface is immersed in a poly acrylic acid (PAA) solution, and immediately after is slowly removed from the solution allowing it to properly dewet the surface and assemble within the wettable patterns. Upon solvent evaporation, the polymer deposits, remaining strictly confined within the pattern recreating their exact shape. Afterwards, the dip-coating and solvent evaporation processes are repeated once more, but instead, using a poly-ε-caprolactone (PCL) solution to build-up the second layer. The dewetting is strongly influenced by the viscosity of a solution[22] and, therefore, different velocities must be applied when using different polymer solutions. The stacking of different polymeric layers is possible since the solvent in which PCL was prepared does not affect the previous one. The sequential deposition of both polymers was confirmed through fluorescence microscopy, where the PAA solution was loaded with Coumarin-6, and the PCL solution with Nile Red (Fig. III.1a). In order to yield freestanding PCL microparticles a single trigger event was employed, *i.e.* immersion in an extremely basic solution of sodium hydroxide (1M NaOH). Due to the pH-responsiveness of the PAA, the NaOH effectively etched and disintegrated the sacrificial layer (PAA), leading to the release of PCL microparticles from the glass substrate into the solution[24,25]. To quicken the process, a mild mechanical stimulation such as agitation or simply creating a flow while pipetting the solution up-and-down can be applied. The dimension and shape of the particles is dictated by the wettable pattern, and thus by the photomask design. Taking this into consideration it was possible to produce, both on-chip and freestanding, particles with different sizes (ranging from 50 to 500 μm) and geometric shapes, including squares, circles, triangles and hexagons (Fig. III.1b, Fig. S1, Supporting Information). This method is suited for the formation of sharped-edge particles, where the definition of the corners is maintained even after detachment. Furthermore, to validate the polymer-wise versatility of this technique, we also fabricated freestanding polystyrene (PS) microparticles, applying the same

conditions for polymer deposition and detachment (Fig. S1, Supporting Information).

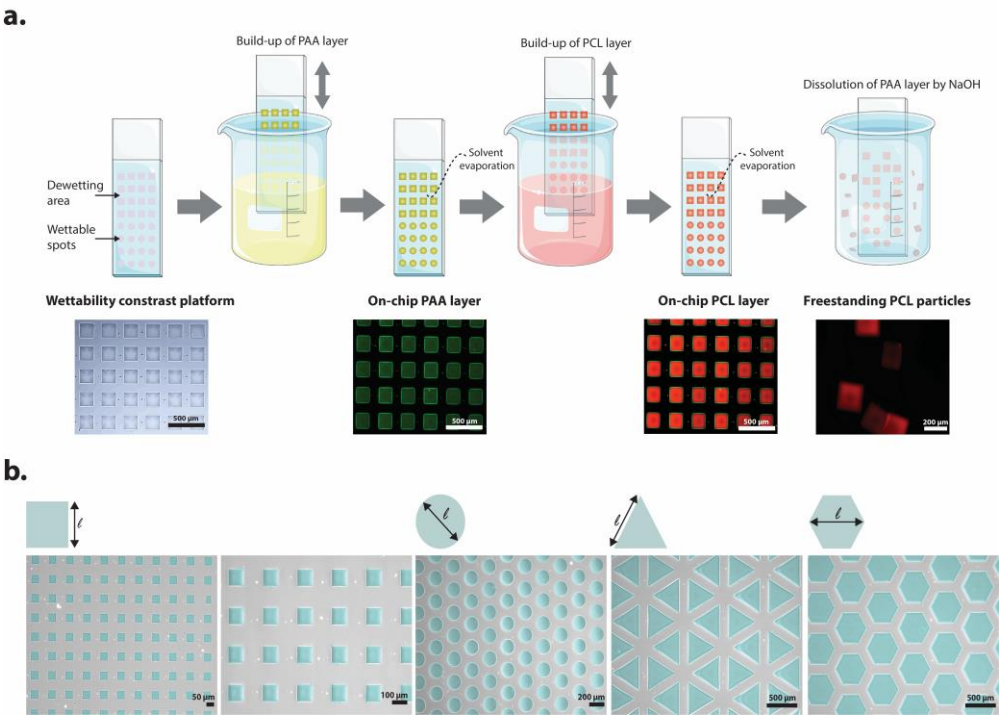

Figure 1. a) Schematic representation of the overall experimental procedure for the fabrication of quasi-2D PCL microparticles. The first step encompasses the dip-coating of the surface in a PAA solution, which upon solvent evaporation and polymer deposition, creates the sacrificial layer. Then, the step is repeated using, instead, a PCL solution to form a new layer on top of the underlying one made out of PAA. Both polymer solutions were stained with different dyes (PAA with Coum-6 and PCL with Nile Red) and assessed by fluorescence microscopy to confirm the deposition and correct overlay between the layers. **b)** Assessing the versatility of the developed platform in generating microparticles portraying different sizes and geometries. Each "ℓ" represented in every image indicates the lateral-size defined to measure particle length. All the acquired images were false-colored using MountainsLab Premium v8.0 software.

III.4. Morphometric analysis of on-chip and freestanding particles

The morphology and topography of both circular and square particles with lateral sizes of 200 μm, on-chip and freestanding, was performed by profilometry analysis. First, to quantitatively assess the fidelity of the polymer pinning efficiency within the patterned domains and, thus, to evaluate the precise and accurate deposition over the edges and the recreation of the pattern, two different approaches were employed: (i) measurement of

the size of the particles - diameter for circles and side dimension for squares (Fig. III.2a), and (ii) measurement of the shape, roundness for circles and aspect ratio for squares (Fig. III.2b)[26]. On-chip particles showed over 95% fidelity for both circles and squares, which indicates that polymer deposition can recreate with great accuracy the chemically imprinted pattern. In turn, for the freestanding particles the fidelity scores slightly decreased, showing around a 93% fidelity, and particle dimensions became more scattered. This dispersion in size may be associated with the NaOH treatment used to detach the particles from the surface, as the NaOH hydrolyzes ester bonds, hence, slightly degrading the PCL structure[27]. Similarly, a shape fidelity over 97% was obtained for on-chip particles, while freestanding particles displayed a less than 3% decrease. This clearly demonstrates the efficiency of the method to produce particles with very precise shapes with well-defined and sharped edges as in the case of the squares (Fig. III.2c). Along with this analysis, the thickness of the materials was measured in three different stages: (i) the deposition of the sacrificial layer, (ii) the build-up of both polymers (deposition of PAA + PCL) and (iii) the PCL particles alone as freestanding objects. Two distinct regions – edges and center - were measured for these three different conditions, as the deposition of the polymer was not uniformly distributed throughout the pattern. Initially, the thickness profile of polymer solutions within the patterned domains is convex due to liquid droplet morphology. Conversely, upon solvent evaporation the profile exhibited displays a concave morphology. This phenomenon is known as the coffee-ring-like effect, and describes how the evaporation of the droplet occurs and how it influences polymer deposition. An enhanced evaporation rate is observed at the droplet edge, which leads to an outward flow of the solvent, driving the movement of solutes towards the contact line and creating a ring-shaped deposition[28]. For this analysis presented here the average thickness was considered and calculated as the arithmetic mean between the maximum value found within the edges and the minimum value in the center. In the case of PAA deposition, the measured thickness is significantly higher ($p < 0.0001$) for squares (ca. 80 nm) comparatively with circles (ca. 60 nm) (Fig. III.2d). This substantial change can be explained by the differences in area that both patterned geometries exhibit. The area displayed by the square patterns is higher than the circular ones, thus, square patterns have the capacity to hold a larger droplet, therefore containing more solute. Concerning the deposition of PCL over the sacrificial layer, three different concentrations were used (2%, 3.5%, 5% (w/v)). A general tendency shows that the particles' thickness increased with the increase in polymer concentration, both for circular and square geometries (Fig.

III.2e). Moreover, the particles' morphology displays a decrease of the coffee-ring effect with increasing PCL concentration. The interval in thickness ranges from ca. 100 nm up to ca. 300 nm, for the lowest and highest PCL concentration, respectively. Therefore, both thickness and topography can be tailored by playing with polymer concentration. To evaluate the thickness of the freestanding structures, it was only considered and quantified the 5% (w/v) PCL condition since were easier to handle, displayed the highest thickness and a less prominent coffee-ring effect (Fig. III.2f). Both geometries show an approximately 200 nm thickness exhibiting a polydispersity index (PDI) of 0.038 and 0.033, for circles and squares, respectively, which reveals a highly monodisperse distribution[29] (Fig. III.2g). The morphology of circles and squares, concerning all of the conditions measured, is highlighted in the Figure 2h. Additionally, to investigate the possibility to further manipulate and tune particle thickness, a sequential dipping strategy was adopted. In this sense, two different solvents with contrasting solubility degrees regarding PCL were used: dichloromethane (high solubility) and acetone (low solubility). Although it is possible to alter the overall thickness through deposition-dissolution, this method reveals to be inconsistent, once the increase of the number of dippings is not fully translated in an increase in thickness (Fig. S2, Supporting Information).

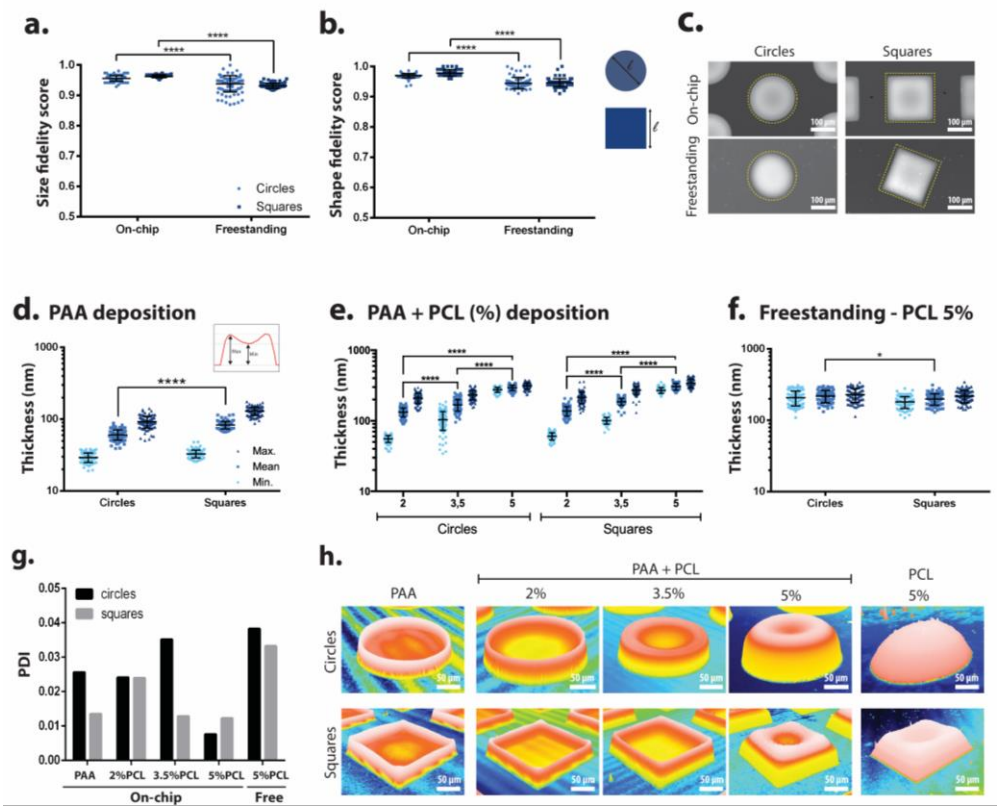

(see the figure legend at the beginning of the next page)

Figure 2. Morphometric characterization and topographic analysis of both circular and square particles (l = 200 μm). **a)** Size fidelity score of on-chip and freestanding particles. **b)** Shape fidelity score of on-chip and freestanding particles (roundness of a perfect circle = 1, and aspect ratio of a perfect square = 1) **c.** Top-views of on-chip and freestanding particles with an overlapping dashed-line shape (yellow) of a perfect l = 200 μm circle and square. **d)** Thickness of the PAA deposition. The inset represents the estimation of the thickness for all of the conditions: the mean values were obtained as an arithmetic mean between the maximum and the minimum values. **e)** Thickness of PAA overlaid with PCL (2%, 3.5%, 5% (w/v)) deposition. **f)** Thickness of freestanding PCL 5% (w/v) microparticles. A minimum of 75 particles were considered and analyzed *per* condition. **g)** Polydispersity index (PDI) of the thickness measured for all of the conditions indicates that all the particles are highly monodisperse (PDI < 0.05)[29]. **h)** Isometric views of the on-chip and freestanding particles, revealing the major morphological and topographical differences. For the statistical analysis the data is presented as mean ± s.d. (n>75) and it is considered statistically different when * $p < 0.05$ and **** $p < 0.0001$.

III.5. *In vitro* performance of hASCs spheroids containing sheet-like particles

To explore the behavior of these materials in contact with cells, the 3D cell aggregates spontaneously self-assembled into spheroids using a round-bottom shaped ultra-low surface adhesion culture plate by solely exposing them to gravitational forces. These gravity-enforced spheroids of human adipose-derived stem cells (hASCs), at a density of 10^4 cells *per* well, were generated with cells only (controls) or embedding PCL particles, 30-50 *per* well (Fig. III.3a). Following 24h of culture, spheroid formation was easily monitored over time using optical microscopy (Fig. III.3b). Both 3D hASCs aggregates alone and the aggregates containing particles show identical diameters, ca. 500 μm for day 1 decreasing to ca. 300 μm for day 3 (Fig. III.3c), probably due to the continued exposure to gravity. This structural compactness overtime creates spheroids with a more circular morphology and similar roundness characteristics (Fig. S3, Supporting Information), highlighting that particles do not compromise the typical spheroid formation, conceivably by their ultrathin thickness. Moreover, PCL particles hydrophilization causes the carboxylated groups at the surface to be exposed, therefore increasing its surface energy necessary to cells to recognize and adhere to it[27]. Upon cell

adherence and spheroid formation, the particles are effortlessly twisted by the cells due to their ultra-thinness and not-stiff morphology. Such uncommonly feature creates a bidirectional culturing concept, where not only the particles are very important key players to dictate cell fate, but also cells are able to manipulate and control the scaffolding material according to their liking, conversely to the classic conception that only the material will dictate the outcome of the cells. An in-depth view at the cross-section of the spheroids under SEM (Fig. III.3d) depicts a moderate roughness in the interior of both conditions, seemingly caused by a densely-packed cells during spheroid compaction. Throughout the inner surface of the spheroid, quasi-transparent structures are observed which likely resemble the particles, highlighting their distribution within the aggregate. The Live/Dead staining of the spheroids with Calcein-AM and Propidium Iodide (Fig. S4, Supporting Information) unveil that cells remain viable both at day 1 and day 3, independently of the presence of particles within the cell aggregate. Due to insufficient oxygen diffusion and nutrient exchange with outer cell culture medium, both spheroids exhibit the expansion of a necrotic core overtime. On the other hand, inspecting the metabolic activity (Fig. III.3e), the cells seem metabolically active in both conditions; however, at day 3, this activity showed a 2-fold increase and is statistically higher ($p < 0.05$) in the spheroid containing particles in comparison with controls. Moreover, in the case of spheroids, containing particles, labelled with phalloidin for cytoskeleton staining and DAPI for nuclei, the majority of the cells, particularly at day 3, display a more elongated morphology rather than a round shape as observed in the controls, highlighting that the support provided by the particles during spheroid formation is somehow key for cell spreading (Fig. III.3f). Although similar in size, the spheroids become to establish a polarized surface layer and unorganized core of cells in the center, as illustrated when they were cross-sectioned after 3 days in culture (Fig. III.3g). Despite a seemingly well-distributed particles within the aggregates (Fig. III.3g, Fig. S5, Supporting information), the internal cells localized at the core of the spheroid are constantly exposed to compressive forces from the coalescence of the neighboring cells, which may induce a more hypoxic environment, due to limited oxygen and nutrient diffusion to the core. However, in spheroids containing particles, the levels of VEGF released from hASCs (Fig. III.3h) are significantly higher both at day 1 ($p < 0.001$) and day 3 ($p < 0.01$) in comparison to cell spheroids alone, which can prominently improve their survival[30]. Probably due to alteration in oxygen metabolic signaling resulting from cell-cell, cell-particle and cell-ECM interactions, hASCs in aggregates containing particles may be able

to increase VEGF secretion, and circumvent and adapt to such hypoxic conditions, eventually preserving to some extent their viability and function[31].

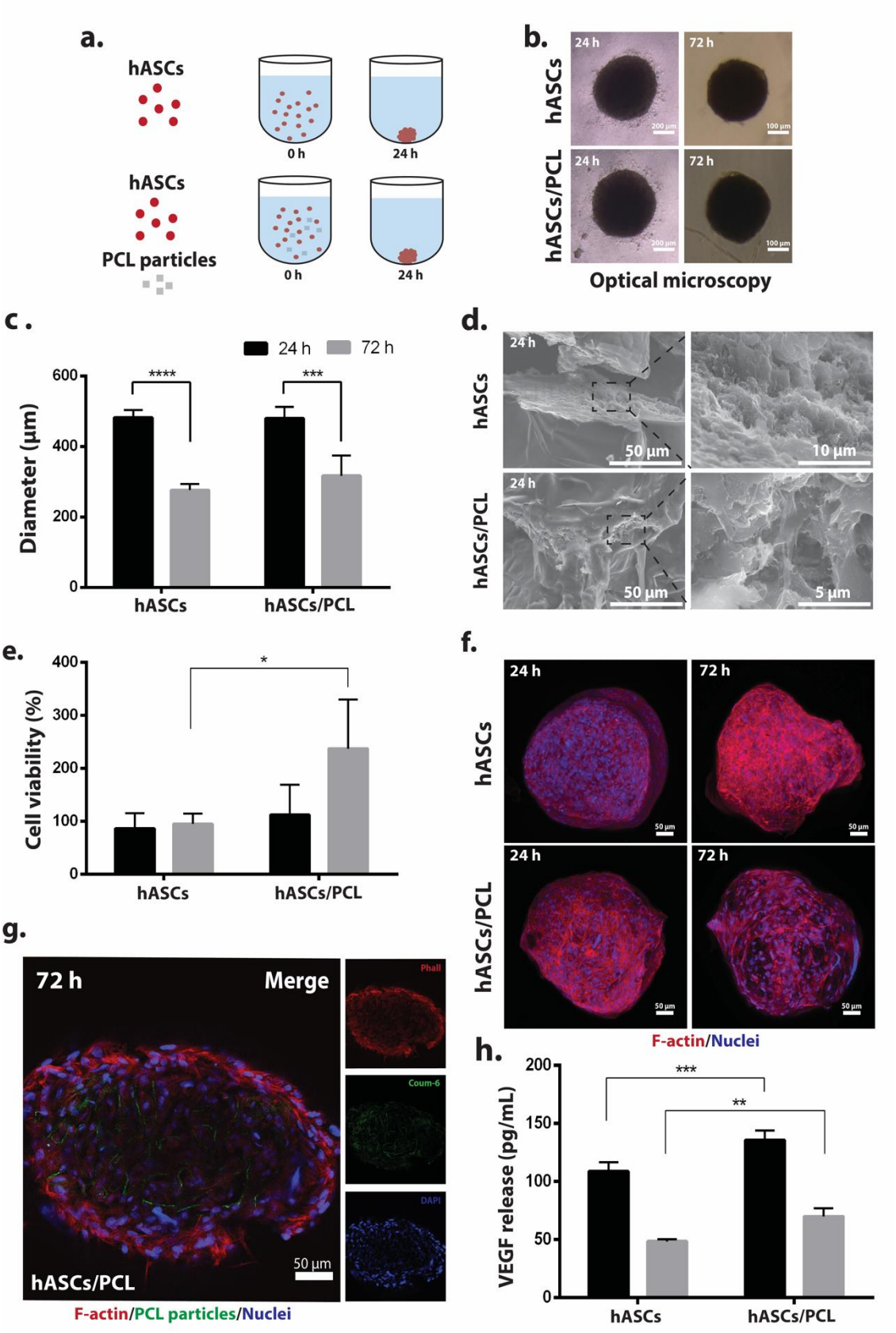

(see the figure legend at the beginning of the next page)

Figure 3. *In vitro* biological performance of sheet-like particles within hASCs spheroids. **a)** Schematic representation of the culture parameters used to assemble hASCs spheroids. **b)** Optical microscopy images of hASCs and hASCs/PCL spheroids at different time-points. **c)** Spheroid diameter assessment along time-points using ImageJ Software analysis (v1.52n). **d)** SEM micrographs of cross-sectioned hASCs and hASCs/PCL spheroids after 24h of culture. **e)** Fluorescence microscopy micrographs of hASCs and hASCs/PCL spheroids of Live/Dead staining (Green channel: Calcein-AM, red channel: PI). **f)** Metabolic activity assessment through AlamarBlue™ assay at 24h and 72h. **g)** CLSM micrographs of hASCs and hASCs/PCL spheroids after 24 and 72 h of culture. Red channel: Flash Phalloidin™ Red 594, blue channel: DAPI. **h)** CLSM micrograph of a cross-sectioned hASCs/PCL spheroid, illustrating the particle distribution within the aggregate at day 3. Cells are stained with Flash Phalloidin™ Red 594 (red channel) and DAPI (blue channel), while the particles are stained with Coum-6. **i)** Quantification of secreted VEGF (pg mL^{-1}) into the medium by hASCs and hASCs/PCL spheroids at both times-points. For the statistical analysis the data is presented as mean ± s.d. (n=4) and it is considered statistically different when * $p < 0.05$, ** $p < 0.01$, *** $p < 0.001$ and **** $p < 0.0001$.

In summary, we demonstrate the fabrication of ultrathin sheet-like particles encompassing a vast array of geometries with high precision and definition in an upfront and large-scalable manner. The method described here is compatible with different types of materials, either for the sacrificial or the freestanding "to be" layers. Moreover, the overall thickness of the freestanding particles is simply controlled by polymer concentration. Gravity-enforced spheroids containing these quasi-2D particles show enhanced metabolic activity, without hindering the typical spheroid formation, morphology and morphometric features. The cell-particle structures can also act as a platform for the release of angiogenic factors, such as VEGF. Additionally, due to the extremely softness of these particles, cell spheroid microenviroment is highly dictated by cells, which, as an almost "biomaterialess" approach, becomes quite appealing as these particles can be engineered with physical and/or chemical moieties to trigger specific cell functions[32].

III.6. References

1. Yang, J., Zeng, Z., Kang, J., Betzler, S., Czarnik, C., Zhang, X., Ophus, C., Yu, C., Bustillo, K., Pan, M., Qiu, J., Wang, L.-W. & Zheng, H. Formation of two-dimensional transition metal oxide nanosheets with nanoparticles as intermediates. *Nat. Mater.* **18**, 970–976 (2019).

2. Bolotsky, A., Butler, D., Dong, C., Gerace, K., Glavin, N. R., Muratore, C., Robinson, J. A. & Ebrahimi, A. Two-Dimensional Materials in Biosensing and Healthcare: From in Vitro Diagnostics to Optogenetics and beyond. *ACS Nano* **13**, 9781–9810 (2019).

3. Zhang, W., Yu, J. & Chang, H. Two dimensional nanosheets as conductive, flexible elements in biomaterials. *J. Mater. Chem. B* **3**, 4959–4964 (2015).

4. Kim, J., Campbell, A. S., de Ávila, B. E. F. & Wang, J. Wearable biosensors for healthcare monitoring. *Nature Biotechnology* vol. 37 389–406 (2019).

5. Lee, S., Yeom, B., Kim, Y. & Cho, J. Layer-by-layer assembly for ultrathin energy-harvesting films: Piezoelectric and triboelectric nanocomposite films. *Nano Energy* **56**, 1–15 (2019).

6. Wang, P., Liu, J., Chen, X., Ma, X., Guo, D., Li, Z. & Pan, J. Janus silica nanosheets-based MMIPs platform for synergetic selective capture and fast separation of 2′-deoxyadenosine: Two different components segmented on the surface of one object. *Chem. Eng. J.* **369**, 793–802 (2019).

7. Inam, M., Jones, J. R., Pérez-Madrigal, M. M., Arno, M. C., Dove, A. P. & O'Reilly, R. K. Controlling the Size of Two-Dimensional Polymer Platelets for Water-in-Water Emulsifiers. *ACS Cent. Sci.* **4**, 63–70 (2018).

8. Pensabene, V., Taccola, S., Ricotti, L., Ciofani, G., Menciassi, A., Perut, F., Salerno, M., Dario, P. & Baldini, N. Flexible polymeric ultrathin film for mesenchymal stem cell differentiation. *Acta Biomater.* **7**, 2883–2891 (2011).

9. Chen, S., Peng, S., Sun, W., Gu, G., Zhang, Q. & Guo, X. Scalable Processing Ultrathin Polymer Dielectric Films with a Generic Solution Based Approach for

Wearable Soft Electronics. *Adv. Mater. Technol.* **4**, 1800681 (2019).

10. Fujie, T., Mori, Y., Ito, S., Nishizawa, M., Bae, H., Nagai, N., Onami, H., Abe, T., Khademhosseini, A. & Kaji, H. Micropatterned Polymeric Nanosheets for Local Delivery of an Engineered Epithelial Monolayer. *Adv. Mater.* **26**, 1699–1705 (2014).

11. Liu, Y., Genzer, J. & Dickey, M. D. "2D or not 2D": Shape-programming polymer sheets. *Prog. Polym. Sci.* **52**, 79–106 (2016).

12. Huang, G. & Mei, Y. Assembly and Self-Assembly of Nanomembrane Materials-From 2D to 3D. *Small* **14**, 1703665 (2018).

13. Callens, S. J. P. & Zadpoor, A. A. From flat sheets to curved geometries: Origami and kirigami approaches. *Mater. Today* **21**, 241–264 (2018).

14. Yin, T., Yang, Z., Lin, M., Zhang, J. & Dong, Z. Preparation of Janus nanosheets via reusable cross-linked polymer microspheres template. *Chem. Eng. J.* **371**, 507–515 (2019).

15. Okamura, Y., Kabata, K., Kinoshita, M., Saitoh, D. & Takeoka, S. Free-Standing Biodegradable Poly(lactic acid) Nanosheet for Sealing Operations in Surgery. *Adv. Mater.* **21**, 4388–4392 (2009).

16. Okamura, Y., Kabata, K., Kinoshita, M., Miyazaki, H., Saito, A., Fujie, T., Ohtsubo, S., Saitoh, D. & Takeoka, S. Fragmentation of Poly(lactic acid) Nanosheets and Patchwork Treatment for Burn Wounds. *Adv. Mater.* **25**, 545–551 (2013).

17. Borges, J. & Mano, J. F. Molecular Interactions Driving the Layer-by-Layer Assembly of Multilayers. *Chem. Rev.* **114**, 8883–8942 (2014).

18. Endo, H., Kado, Y., Mitsuishi, M. & Miyashita, T. Fabrication of Free-Standing Hybrid Nanosheets Organized with Polymer Langmuir−Blodgett Films and Gold Nanoparticles. *Macromolecules* **39**, 5559–5563 (2006).

19. Fujie, T. Development of free-standing polymer nanosheets for advanced medical and health-care applications. *Polym. J.* **48**, 773–780 (2016).

20. Taccola, S., Desii, A., Pensabene, V., Fujie, T., Saito, A., Takeoka, S., Dario, P.,

Menciassi, A. & Mattoli, V. Free-Standing Poly(l -lactic acid) Nanofilms Loaded with Superparamagnetic Nanoparticles. *Langmuir* **27**, 5589–5595 (2011).

21. And, J. E. C. & Huck, W. T. S. Formation of Hybrid 2D Polymer−Metal Microobjects. *Langmuir* **23**, 1569–1576 (2007).

22. Kobaku, S. P. R., Kwon, G., Kota, A. K., Karunakaran, R. G., Wong, P., Lee, D. H. & Tuteja, A. Wettability Engendered Templated Self-assembly (WETS) for Fabricating Multiphasic Particles. *ACS Appl. Mater. Interfaces* **7**, 4075–4080 (2015).

23. Feng, W., Li, L., Du, X., Welle, A. & Levkin, P. A. Single-Step Fabrication of High-Density Microdroplet Arrays of Low-Surface-Tension Liquids. *Adv. Mater.* **28**, 3202–3208 (2016).

24. Gao, Y., Xu, W. & Serpe, M. J. Free-standing poly (N-isopropylacrylamide) microgel-based etalons. *J. Mater. Chem. C* **2**, 5878–5884 (2014).

25. Swift, T., Swanson, L., Geoghegan, M. & Rimmer, S. The pH-responsive behaviour of poly(acrylic acid) in aqueous solution is dependent on molar mass. *Soft Matter* **12**, 2542–2549 (2016).

26. Yu, H., Lim, K. P., Xiong, S., Tan, L. P. & Shim, W. Functional morphometric analysis in cellular behaviors: Shape and size matter. *Advanced Healthcare Materials* vol. 2 1188–1197 (2013).

27. Nguyen, L. T. B., Odeleye, A. O. O., Chui, C. Y., Baudequin, T., Cui, Z. & Ye, H. Development of thermo-responsive polycaprolactone macrocarriers conjugated with Poly(N-isopropyl acrylamide) for cell culture. *Sci. Rep.* **9**, 3477 (2019).

28. Mirbagheri, M. & Hwang, D. K. The Coffee- Ring Effect on 3D Patterns: A Simple Approach to Creating Complex Hierarchical Materials. *Adv. Mater. Interfaces* **6**, 1900003 (2019).

29. Danaei, M., Dehghankhold, M., Ataei, S., Hasanzadeh Davarani, F., Javanmard, R., Dokhani, A., Khorasani, S. & Mozafari, M. R. Impact of particle size and polydispersity index on the clinical applications of lipidic nanocarrier systems. *Pharmaceutics* vol. 10 (2018).

30. Seo, J., Lee, J. S., Lee, K., Kim, D., Yang, K., Shin, S., Mahata, C., Jung, H. B., Lee, W., Cho, S.-W. & Lee, T. Switchable Water-Adhesive, Superhydrophobic Palladium-Layered Silicon Nanowires Potentiate the Angiogenic Efficacy of Human Stem Cell Spheroids. *Adv. Mater.* **26**, 7043–7050 (2014).

31. Guaccio, A., Guarino, V., Perez, M. A. A., Cirillo, V., Netti, P. A. & Ambrosio, L. Influence of electrospun fiber mesh size on hMSC oxygen metabolism in 3D collagen matrices: Experimental and theoretical evidences. *Biotechnol. Bioeng.* **108**, 1965–1976 (2011).

32. Neto, M. D., Oliveira, M. B. & Mano, J. F. Microparticles in Contact with Cells: From Carriers to Multifunctional Tissue Modulators. *Trends Biotechnol.* **37**, 1011–1028 (2019).

Chapter IV

General Conclusions and Future Perspectives

Strategies encompassing the use of microparticles have been extensively and almost exclusively used as spherical carriers for controlled drug delivery systems and for the large scale cellular expansion. Even though, they have been increasingly integrated in more unconventional and sophisticated strategies, such as the bottom-up tissue engineering, 3D bioprinting, or even in the development of 3D tissue and disease models. The traditional concept of the "dull" bulk spherical particle is slowly being replaced and reestablish, as more advanced and versatile designs can elevate and upgrade particle performance only by modulating its (bio)chemical and physical properties. Among several displayed physical features, size and geometry have a highly impact on shaping their overall function. In this sense, simply by narrowing the dimensions and enhanced surface area, quasi-2D structures have proven a tremendous relevance in countless fields due to their unique properties.

The fabrication of low dimensional materials is compatible with multiple technologies, but pre-patterned platforms, such as the ones exhibiting extreme wettability domains, offer control over lateral dimensions and overall shape. Bearing this in mind, the work envisioned the development of a method based on wettability contrasts platforms to produce quasi-2D polymeric particles with tunable sizes and geometries. The method proved to be fast, simple and straightforward, compatible with large-scalability, rendering multiple particles at a time. Although compatible with different types of materials, this platforms only work with polymers soluble in organic solvents, excluding water-soluble and natural-origin polymers. On the other hand, shows a great efficiency in generating particles with high precision and definition, yielding particles from 50 to 500 μm in size, and very sharped-edge geometries, such as squares, triangles and hexagons. Moreover, the particles exhibit a nanometer-scale thickness which results in a very soft, rather than stiff material, and highly flexible structure. This highly pliable material could be employed in strategies based on origami-like structures and find new potentialities. Nonetheless, they can still hold their shape and structure integrity when in their freestanding state.

Gravity-enforced spheroids containing these quasi-2D particles show enhanced metabolic activity, without hindering the typical spheroid formation, morphology and morphometric features. The particles are homogeneously embedded within the aggregate and cells easily twist, fold and bend them according to their liking, while acting as supporting matrices. This bidirectional culturing approach allows not only the material to dictate cell fate, but also offers the cell enough freedom to participate and modulate their

own outcome. Furthermore, the cell-particle structures can also act as a platform for the release of angiogenic factors, namely VEGF. Such enriched medium could work as a conditioned medium to supplement other VEGF-needy cell lines.

Additionally, due to the extremely softness of these particles, cell spheroid microenviroment is highly dictated by cells, which, as an almost “biomaterialess” approach, becomes quite appealing as these particles can be engineered with physical and/or chemical moieties to trigger specific cell functions.

Support Information

S1. Different geometries and sizes of on-chip and freestanding particles.

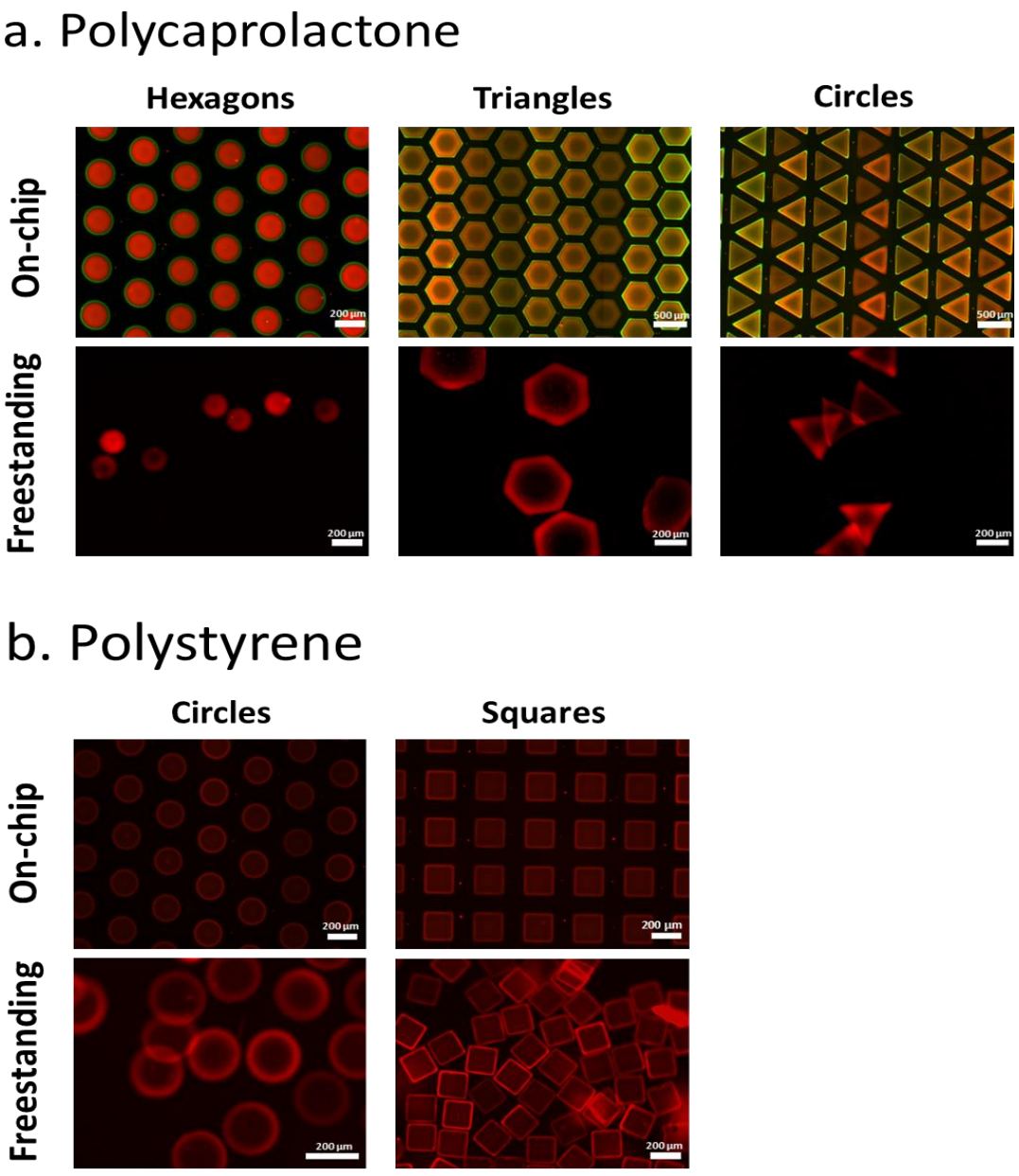

Figure S1. Fluorescence microscopy of the different geometries and sizes on-chip and freestanding particles. **a)** PCL particles. PAA was stained with Coum-6 (green channel) and PCL with Nile red (red channel). **b)** PS particles were stained with Nile red (red channel).

S2. Assessment of the thickness influenced by the sequential number of dip-coatings on on-chip particles using different solvents.

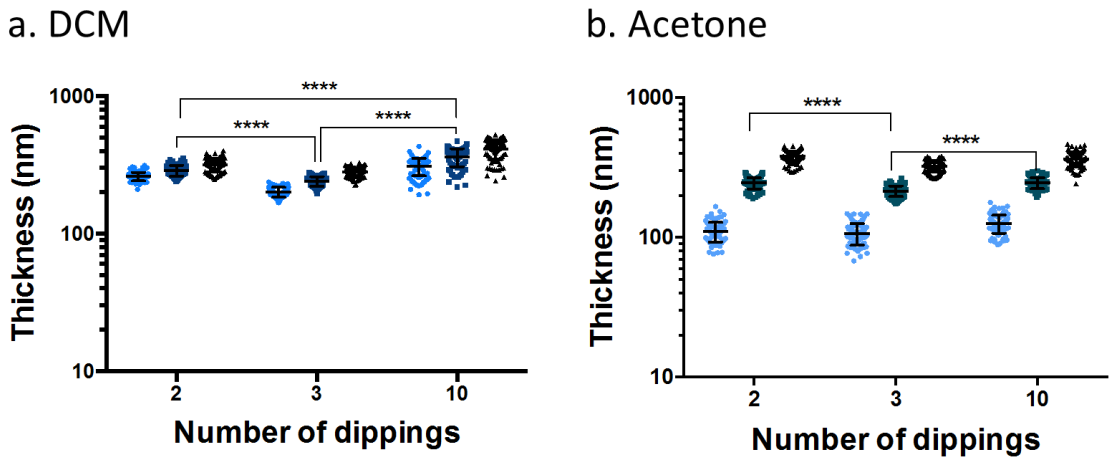

Figure S2. Evaluation of thickness behavior upon increase of the number of sequential dippings in 5 % (w/v) PCL solution in **a)** DCM (high solubility) and **b)** Acetone (low solubility). Data regarding 200 μm diameter circles. Statistical analysis: Data is presented as mean ± s.d (n>75) **** $p < 0.0001$.

S3. Morphometric analysis of spheroids generated with hASCs alone (hASCs) and hASCs containing PCL particles (hASCs/PCL).

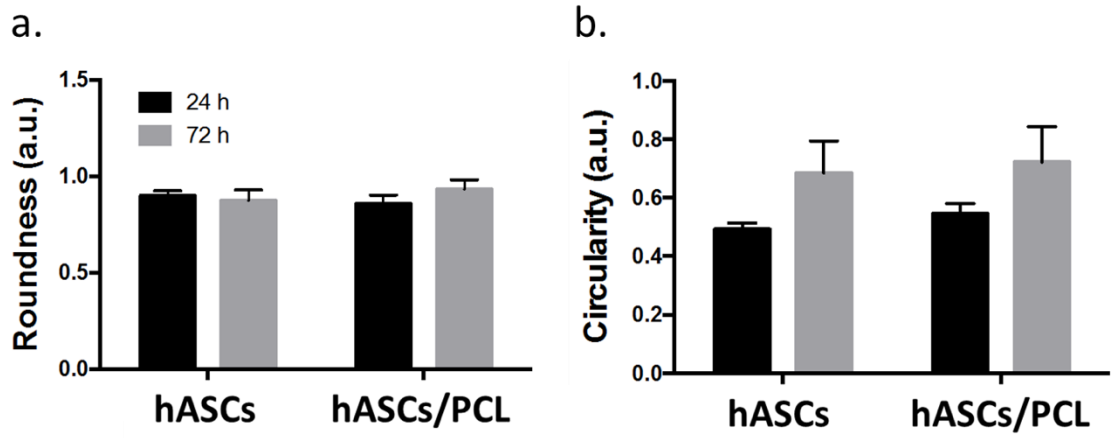

Figure S3. Spheroid morphometric features through ImageJ software analysis. **a)** roundness **b)** circularity.

S4. Live/Dead staining of hASCs and hASCs/PCL spheroids.

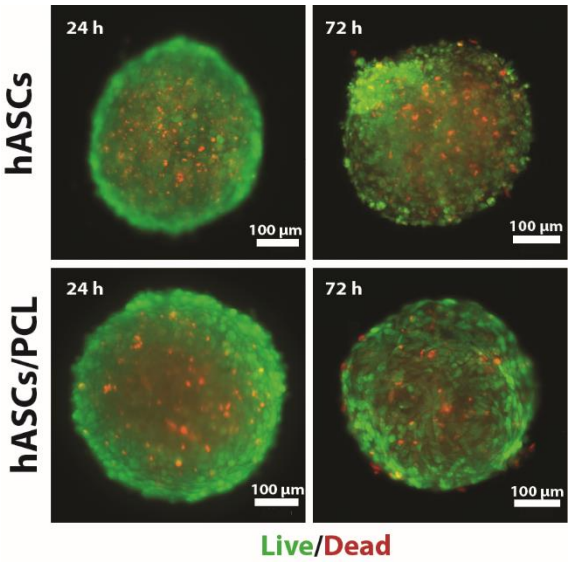

Figure S4. Fluorescence microscopy micrographs of Live/Dead staining of hASCs and hASCs/PCL spheroids. The staining was performed with Calcein-AM (green channel) and PI (red channel).

S5. Twisting of PCL particles by MC3T3-E1 cells

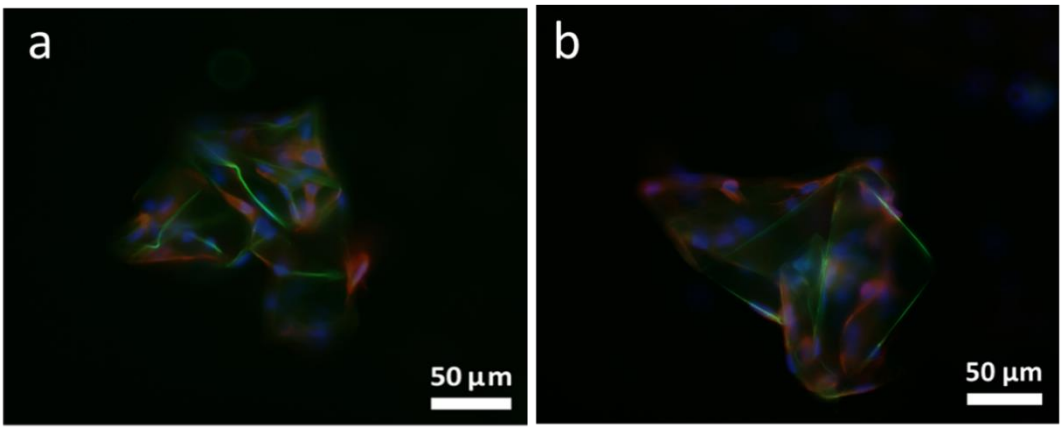

Figure S5. Evidence of the ultra-thinness and soft nature of PCL microparticles upon contact with cells. (**a, b)** MC3T3-E1 folding a l = 200 µm square particle, originating origami-like structures guided by cells. PCL microparticles were stained with Coum-6, F-actin with Flash Phalloidin^{TM} Red 594, and nuclei with DAPI.